Facies architecture, hydrostratigraphy, and aquifer characterization of Quaternary alluvium adjacent to Yucca Mountain, Nevada

Ressler, T.R.
Groundwater Solutions, Inc., 55 SW Yamhill Street, Suite 400, Portland, Oregan 97204, USA

Ridgway, K.D.
Department of Earth and Atmospheric Science, Purdue University, West Lafayette, Indiana 47907, USA

Stamatakos, J.A.
J. Winterle
Center for Nuclear Waste Regulatory Analyses, Southwest Research Institute®, San Antonio, Texas 78238, USA

Sharp, J.M., Jr.
Department of Geological Sciences, The University of Texas at Austin, Austin, Texas 78712, USA

ABSTRACT

Quaternary alluvium in sedimentary basins adjacent to Yucca Mountain, Nevada, USA, may be more than 1,000 m thick. The modern entrenched channel of Fortymile Wash, a large desert wash located east-southeast of Yucca Mountain, provides several laterally continuous, well-exposed outcrops of the alluvium. Aquifer characterization of these outcrops provides the best available analog of the subsurface alluvial aquifer down gradient from Yucca Mountain.

Eight diagnostic sedimentary facies are identifiable in the alluvium of Fortymile Wash based on grain size, sedimentary structures, and geometry. The facies architecture of the alluvium is characterized by conglomeratic, braided channel facies that are on the order of 10 m thick. Channel facies are interbedded with tabular, sandy paleosol facies that are on the order of 1–2 m thick. Hydraulic estimates for the different facies were developed from laboratory permeameter tests and from empirical relations based on the results of grain-size analyses. These data provide a framework to understand the spatial heterogeneity and distribution of aquifer properties. Estimates of total porosity in the eight facies range from 0.21 to 0.42, with the coarser-grained channel facies having lower porosities than the finer-grained paleosol facies. Hydraulic conductivity within the alluvium varies over at least three orders of magnitude, based on our measurements. The least permeable facies in the alluvium are paleosol facies, which are commonly laterally extensive for hundreds of meters and consequently may form important vertical flow barriers in the alluvial aquifer. The most permeable facies are channel facies of horizontally stratified conglomerate and sandstone, which also are the volumetrically dominant facies observed in outcrop. Our new sedimentary facies and hydraulic properties data suggest the interlayering of more permeable channel facies with less

permeable paleosol facies may stratify and compartmentalize groundwater flow through the alluvial aquifer.

INTRODUCTION

One component in the evaluation of Yucca Mountain as a potential repository for safe disposal of high-level waste is groundwater flow in the saturated zone, from beneath the repository footprint to 36° 40′ 13.6661″ north latitude in the predominant direction of the groundwater flow, as defined in 10CFR63.302(1)(i) (Fig. 1A). Located in the northern Amargosa Desert of central Nevada, USA, Yucca Mountain has been recommended by the U.S. Department of Energy (DOE) as the potential site for a permanent geologic repository for high-level waste. Ongoing site characterization at Yucca Mountain includes investigation of saturated zone flow paths from the potential repository area to the specified regulatory compliance boundary located down gradient from Yucca Mountain. Flow paths from the water table beneath Yucca Mountain originate in fractured volcanic tuff in which flow is conceptualized to occur mainly in fracture networks with small effective porosity and, hence, relatively high groundwater velocities. Downstream from Yucca Mountain, flow paths transition from the fractured volcanic tuff aquifer system into an alluvial aquifer system, which is conceptualized to have relatively high effective porosity and proportionally slower groundwater velocity. The distance at which this transition occurs depends on the exact flow path and basin geometry. Total system performance assessment studies of the potential repository suggest groundwater travel through saturated alluvial aquifer may be an important natural barrier to radionuclide migration because of the slower groundwater velocity and greater mineral surface area accessible for radionuclide sorption compared with the fractured tuff.

Site characterization data, principally from the Nye County Early Warning Drilling Program (Nye County, 1999), suggest that predicted flow paths pass through at least some portion of the alluvial aquifer. The distance any potential flow paths might extend through the alluvial aquifer and the thickness of the alluvial aquifer are, at present, uncertain. Oatfield and Czarnecki (1989) estimated that 5 km north of Lathrop Wells Junction (Fig. 1B), the alluvium thickness may exceed 1,000 m based on driller's logs and gravity and resistivity surveys, along the eastern side of Fortymile Wash and juxtaposed to the Down-to-the-West Gravity Fault (Fig. 1B). In addition, geophysical data (gravity and electrical sounding) have identified a gravity low in the Amargosa Valley (Fig. 1A) that extends to the north-northwest across Fortymile Wash, which may represent a thick alluvial aquifer (Snyder and Carr, 1982).

Short-duration pumping tests in Nye County Early Warning Drilling Program Wells 1D, 3D, and 9S (Fig. 1A) yielded transmissivity estimates ranging from 200 to 5,000 m^2/day, but these wells apparently produce water from both alluvial and volcanic tuff aquifers (Nye County, 1999). Additionally, these three wells are all west of the Lathrop Wells volcanic cone (Fig. 1A) and do not intercept likely flow paths from Yucca Mountain (Nye County, 1999). More recently, Nye County Early Warning Drilling Program Wells 2DB, 19P, 19D, 10S, 10P, 22S, and 22PB have been completed along the southern reach of Fortymile Wash. These wells penetrate the alluvial aquifer system in the area where flow paths from Yucca Mountain are projected by groundwater flow models (e.g., Bechtel SAIC Company, LLC, 2003a; Winterle, 2003). Pumping test data from Well 19P indicate moderately high hydraulic conductivity in the range of 0.2–2 m/d [0.7–6 ft/d], based on results from Questa Engineering Corp. (2001) and Reimus and Umari (2002), which are summarized by Winterle and Farrell (2002). Although no pumping test data are available for Wells 2DB, 19D, 10S, 10P, 22S, and 22PB, stratigraphic logs indicate the

presence of coarse sediments likely to have moderate to high hydraulic conductivity, interlayered with low permeability silts and clays.

Estimates of groundwater velocities in the alluvial aquifer down gradient of Yucca Mountain also are necessary to evaluate the efficacy of these units as natural barriers to radionuclide migration. Current conceptual models of the DOE and the U.S. Nuclear Regulatory Commission (NRC) indicate that most attenuation of radionuclides along the flow path will occur within the alluvial aquifer because of (1) significantly slower groundwater velocities compared with the tuff units up gradient, (2) associated high mineral surface area to volume ratios, and (3) advantageous mineral compositions.

We studied facies types, facies architecture, and related hydraulic properties along several outcrops of the alluvium exposed in Fortymile Wash (Fig. 1B) to develop a more realistic understanding of the alluvium in the alluvial aquifer. These outcrops provide unique analogs to the strata within the alluvial aquifer in Fortymile Wash and the Amargosa Desert. The aim of this work is to develop the technical basis needed to evaluate process-level or performance assessment models of groundwater flow in the alluvial aquifer down gradient from Yucca Mountain. In this paper, we provide field observations about the sedimentary characteristics for facies of the alluvium, develop a depositional model for the alluvium to predict geometries of different facies, estimate hydraulic properties for the different facies, and discuss the implications of these new data for groundwater flow through the alluvial aquifer.

PHYSIOGRAPHY, GEOLOGIC SETTING, AND PREVIOUS WORK

Yucca Mountain is located in southwestern Nevada (Fig. 1A) in the Great Basin, of the Basin and Range Province. Structurally, Yucca Mountain is part of a series of north to

north-northeast-trending, fault-bound ridges crossed by occasional northwest-trending strike-slip faults. Stratigraphically, Yucca Mountain consists of a thick accumulation of Cenozoic volcanic tuffs deposited on an irregular surface of eroded and deformed Paleozoic and Precambrian strata. Yucca Mountain is bounded by actively subsiding sedimentary basins (e.g., Crater Flat, Fortymile Wash/Jackass Flats, and Amargosa Valley) (Fig. 1A) currently being filled with alluvium and aeolian strata by alluvial-fan, braided-stream, and aeolian depositional systems. The best exposures of the alluvium are in Fortymile Wash, located east of Yucca Mountain (Fig. 1B). Fortymile Wash is the largest tributary of the upper Amargosa River and is one of the largest alluvial systems in the Southern Basin and Range Province (Glancy and Beck, 1998; Lundstrom et al., 1998). Fortymile Wash extends south-southwest from Yucca Mountain into the Amargosa Valley and is rimmed in its upper reaches by comparatively small transverse alluvial fans emerging from the surrounding uplands (Fig. 1A and 1B). The active wash channel is entrenched to depths exceeding 20 m and gently grades into a wide alluvial plain within the Amargosa Valley immediately north of U.S. Highway 95 (Fig. 1B).

A limited number of geomorphic studies describe the development of alluvial soils in the Fortymile Wash/Yucca Mountain region using soil pit and surface observations and map the surficial alluvial units using surface features, soil morphology, and geochronology (Paces et al., 1994; Lundstrom et al., 1995, 1998). Sedimentological studies of the alluvium in Fortymile Wash are limited to a brief description of an outcrop in the central part of Fortymile Wash (Guertal et al., 1994) and documentation of a debris flow deposit on a transverse alluvial fan bordering Fortymile Wash (Coe et al., 1997).

Similar to much of the Great Basin, Yucca Mountain has a thick (up to 750 m) unsaturated zone (Robinson, 1984), which thins to approximately 100–150 m in southern

Fortymile Wash. The only available site-specific estimate of effective porosity for saturated alluvium along potential Yucca Mountain flow paths is a value of 0.10, based on results from single-well tracer tests at the Alluvial Testing Complex. The results of these small-scale tracer tests, however, also confirm the uncertainty in effective flow porosity because tracer recoveries could be reasonably modeled using a range of effective porosities from 0.05 to 0.3 (Bechtel SAIC Company, LLC, 2003b). Accordingly, this range of uncertainty is considered in the abstraction of saturated zone flow and transport processes for DOE performance assessments of a potential repository at Yucca Mountain. The NRC Total System Performance Assessment Version 4.1j code uses effective porosity values based on estimates of specific yield provided by Walker and Eakin (Mohanty and McCartin, 1998). The Walker and Eakin (1963) values are not based on data from the alluvium south of Yucca Mountain, but are, instead, based on estimates from other sites considered as reasonable analogs. Guertal et al. (1994) provided limited estimates of total porosity and hydraulic conductivity for the nearsurface alluvium of Fortymile Wash based on ponding experiments and on grain-size analyses.

AQUIFER CHARACTERIZATION

Facies

The alluvium of Fortymile Wash was subdivided into distinct facies based on grain size, sedimentary structures, and geometry (e.g., bed thickness, lateral continuity, and such) as summarized in Table 1. These data were then used to determine the depositional process(es) responsible for each of the identified facies. In the subsequent discussions, the term facies is used in the context of sedimentary facies, that is, reflecting the sedimentary origins of the facies. A summary of the facies data and interpreted process(es) of deposition is provided in Table 1.

Facies F1

Description. The most common facies within the alluvium is horizontally to subhorizontally stratified conglomerate and sandstone, here defined as Facies F1 (Fig. 2A). The characteristic feature of the facies is alternating layers or packages of coarse and fine gravel, sometimes referred to as gravel couplets or gravel-sand couplets in the literature (e.g., Folk and Ward, 1957; Smith, 1970, 1974; Miall, 1977; Blair, 1987; Blair and McPherson, 1994; and Todd, 1996). The coarse fraction consists of clast-supported medium gravel to fine cobbles with sand. In some exposures, the coarse fraction has higher concentrations of sand producing a distinctive bimodal grain size content; whereas in other exposures, the coarse fraction lacks any appreciable amount of sand, yielding an open framework (Fig. 2A). The fine fraction consists of interlayered medium to coarse sand and fine gravel. The sand layers tend to be more strongly cemented than the gravelly layers and stand out in relief, highlighting the stratification. These gravel-sand couplets vary in thickness, but are typically less than 50 cm. Imbrication of clasts is common and is particularly evident in the coarser, elongated clasts. Numerous thin (millimeters in thickness) but laterally extensive sandy caliche layers are commonly present in this facies and are characteristically separated by intervals of tens of centimeters. These thin caliche layers are concentrated in the sandier component of the facies and commonly cap the gravel-sand couplets. Minor amounts of low-angle, stratified conglomerate are commonly found in association with the horizontally to subhorizontally stratified conglomerate and sandstone. Facies F1 is found in all of our measured sections, but is best exposed in our Portal 1 measured section (Fig. 3).

Interpretation. The horizontally stratified, alternating layers of conglomerate and sandstone are interpreted as longitudinal bar deposits (e.g., Smith, 1974). Other investigators have noted and described these types of deposits in braided-stream environments (e.g., Folk and

Ward, 1957; Smith, 1970, 1974; Miall, 1977; Todd, 1996) as well as in alluvial-fan environments (Blair, 1987; Blair and McPherson, 1994); although Blair (1987) attributes the formation to the migration of antidunes rather than longitudinal bars. The varying proportion of sand with the gravel has been attributed to discharge fluctuations (Smith, 1974). The open-framework gravels are deposited during high flow when the finer gravel and sand are maintained in suspension. As flow decreases, successively finer gravel is deposited, and, eventually, both gravel and sand are deposited simultaneously (Smith, 1974). The thin, lateral extensive caliche layers within Facies F1 probably reflect when the upper surface of a deposited package of sediment was exposed to subaerial conditions during periods of nondeposition. The low-angle, stratified conglomerate likely represents lateral-foreset deposits formed along the margins of longitudinal bars as flow was dispersed across the bar (e.g., Smith, 1974).

Facies F2

Description. Facies F2 is characterized by clast-supported, well sorted cobble to boulder conglomerate with a matrix of well-cemented medium to coarse sandstone (Fig. 2B). This facies typically has a distinct bimodal grain size consisting of cobbles to boulders and medium to coarse sand. Some clasts are imbricated. Scattered outsized boulder clasts in the range of 60 cm occur. Facies F2 occurs as isolated lenses within Facies F1 with lengths of 10–50 m and thickness of 0.1–1 m (Fig. 3B). The coarsest clasts occur near the center, and the facies commonly grades laterally into better sorted, finer-grained conglomerate. Facies F2 is best developed in the 40mPROX, Portal 1, and 40mBIG measured sections (Fig. 3A,B,C).

Interpretation. Facies F2 is interpreted as channel deposits that formed between longitudinal bars in a braided-stream system (e.g., Miall, 1977). Sedimentary structures in Facies F2 are characteristic of stream-flow deposits. Evidence for stream-flow processes

includes the framework support, imbrication, and lenticular geometries. The organized and imbricated conglomerate clasts of Facies F2 are typical of modern fluvial conglomerate that forms when gravel is transported as bedload and deposited under waning flow by accretion of progressively smaller clasts in channels (Collinson, 1986). Similar, ancient braided-stream facies have been described in many studies (e.g., Ridgway and DeCelles, 1993; Ridgway et al., 1997).

Facies F3

Description. Lenticular units of cross-stratified conglomerate are locally present within the horizontally stratified conglomerate and sandstone of Facies F1 (Fig. 2C). The lenticular units are on the order of 5–15 m in length. Stratification within the lenticular units varies from stratification parallel to the base of the lens, to cross-stratification that is tangential to the base, to tabular planar cross-stratification. A coarse gravel to cobble lag is common along the base of the lenticular units. Facies F3 is not common and is only present in the Portal 1 and 40mBIG measured sections (Fig. 3).

Interpretation. The lenticular units of cross-stratified conglomerate locally present within the horizontally stratified conglomerate are similar to structures observed by Siegenthaler and Huggenberger (1993) in their investigation of Pleistocene braided-stream deposits in Switzerland. Following Siegenthaler and Huggenberger, the lenticular units of cross-stratified gravel are interpreted as scour pool deposits developed at the convergence of two braid channels. A geometric model of pool migration with time and an orientation of a cross-sectional view (i.e., orientation of outcrop) provide an explanation for the differing styles of cross-stratification observed within the lens-shaped units (Siegenthaler and Huggenberger, 1993, Figure 12).

Facies F4

Description. Facies F4 consists of massive, poorly sorted, clast-supported conglomerate that contains diverse grain sizes ranging from sand to boulders with coarse gravel to fine cobbles predominating. Imbrication of clasts is common. This facies sometimes exhibits crude horizontal to subhorizontal stratification highlighted by partitioning of coarser- and finer-grain sizes into crude gravel couplets 40–50 cm thick (Fig. 2D). The finer portions consist of sand to gravel, and the coarser portions consist of sand to cobbles. In some exposures, the cobble layers are strongly cemented and have significant caliche development. Small lenses of sand to fine gravel, typically less than 30 cm thick, are variably present within the facies. Facies F4 occurs in tabular units of 2–3 m thick. Cross-stratified fine to medium conglomerate and sandstone with erosional bases are commonly present at the top of the facies. The crude gravel couplets of Facies F4 are quite similar to those of Facies F1 (except for the larger grain sizes). Further, there appears to be a gradation, rather than a distinct textural break, between Facies F4 and the finer-grained deposits of Facies F1. In cases where it was difficult to differentiate between Facies F4 and F1, we have labeled the facies as "F4 or F1" on our measured sections (e.g., 12.3–15 m on Fig. 3C). Facies F4 was documented in all our measured sections except at Portal 1 (Fig. 3). Facies F4 is particularly well developed in the 40mPROX and 40mMED sections (Figs. 3A, 3B); it composes most of the 40mMED section.

Interpretation. The poor sorting and organization of Facies F4 indicate more turbulent depositional processes, but the presence of crude stratification and clast imbrication indicate that tractive transport processes were still in effect. This facies is interpreted as deposits of turbulent flood flows containing extremely high sediment concentrations. Similar poorly sorted and poorly organized deposits have been described by Nemec and Steel (1984) and attributed to

fluvial sediment flows. Terminology regarding these types of deposits and this realm of fluid flow is not well defined, and according to Nemec and Steel (1984), these types of flows also have been referred to as hyperconcentrated flows, intermediate-type flows, streamfloods, and sheetfloods. The cross-stratified conglomerate and sandstone commonly present atop the facies are interpreted as erosion and deposition by lower discharge channelized flows following the flood flow.

Facies F5

Description. Facies F5 is a matrix- to clast-supported, disorganized deposit consisting of angular gravel to boulders with a matrix of medium to coarse sand (Fig. 2E). The facies has a distinct bimodal sediment content, and the angularity of the clasts strongly contrasts with the predominantly subrounded to rounded textures of the clasts in other facies of the alluvium. The facies is distinctively almost monolithologic in clast composition as well. Some clasts of differing lithology are present in the deposit in minor amounts, but these clasts have the more rounded texture characteristic of the other facies in the alluvium. Facies F5 is extremely rare and was observed in only one bed at the Portal 1 outcrop (at ~1 m on Fig. 3B). In this exposure, the facies is variable in thickness but always less than 1 m and laterally extensive for 10–15 m.

Interpretation. On the basis of the extreme angularity of the clasts, the dominantly monolithologic clast composition, and the disorganized arrangement of the clasts, Facies F5 is interpreted as a sediment gravity flow deposit, in this case, probably a debris flow. The more rounded clasts of differing lithologies contained in the facies are interpreted as alluvium that was deposited within the main channel of Fortymile Wash and subsequently was entrained by the sediment gravity flow. This facies is limited in outcrop exposure and is volumetrically minor in the areas where outcrops are available. This facies, however, may be more volumetrically

important toward the margins of Fortymile Wash where mountains rim the wash: localities with steep slopes where modern sediment gravity flow processes are active, where relict deposits are present, or both (e.g., Coe et al., 1977; Ressler, 2001).

Facies F6

Description. Facies F6 consists of gravel to boulder conglomerate with well developed calcrete cement (Fig. 2F). The facies varies from 5–30 cm in thickness, though typically not exceeding 20 cm. The facies is laterally extensive for hundreds of meters, though varying in thickness and in some cases, locally discontinuous over the length of exposure. Facies F6 is commonly present stratigraphically below Facies F7. These gravelly calcrete horizons stand in relief and form resistive ledges in outcrop. Facies F6 was documented in all our measured sections, but is best developed in Portal 1 (11–14 m on Fig. 3B) and in 40mBIG (10–21 m on Fig. 3C).

Interpretation. Facies F6 is interpreted as part of an ancient soil profile (i.e., paleosol) that represents a subsurface horizon enriched in calcium carbonate. These calcrete-rich horizons likely represent Bk horizons in the paleosol profile (Machette, 1985), and in the paleosol classification of Mack et al. (1993), would be classified as Calcisols because the calcic horizon is the most prominent pedogenic feature. Similar types of deposits, termed calcic soils, are typical of soils throughout much of the arid and semiarid southwestern United States (Machette, 1985). These types of soils have significant accumulations of secondary calcium carbonate and have been well described in alluvial-fan and fluvial deposits (e.g., Gile and Hawley, 1966; Lattman, 1973; VanArsdale, 1982; Allen, 1986; Retallack, 1983; Holliday, 1989).

Facies F7

Description. Facies F7 consists of medium to coarse sandstone with well-developed calcite cement. The facies contains varying concentrations of gravel to cobbles, is mildly to heavily bioturbated (burrowing and root traces), and commonly has small caliche layers within the unit. The internal stratification of the facies is variable. In many units, the internal stratification resembles that of previously defined facies except for the increased sand content, increased cementation and caliche formation, and the reddish color. In other exposures, the facies appears more massive. This facies is often 1–2 m thick and laterally continuous for hundreds of meters along the exposure. In other exposures, the facies consists of discontinuous lenses 0.5–1 m thick and 10–40 m in length that occur at the same stratigraphic position throughout the exposure (Fig. 2G). In general, thicker units tend to be highly bioturbated, completely homogenized (unstratified), and contain scattered gravel to cobble clasts (Fig. 2F). Facies F7 is found in all our measured sections, but is especially well exposed in 40mBIG (e.g., 15–16.2 m and 19.6–20.8 m on Fig. 3C).

Interpretation. The relative fine-grained size, intensive caliche development, calcite cement, bioturbation, and reddish coloration of Facies F7 are consistent with formation by pedogenic processes (e.g., Retallack, 1990; Mack et al., 1993). During prolonged periods of subaerial exposure, alluvium became bioturbated from plant roots, and detrital ferromagnesium minerals were oxidized (reddened) (e.g., Walker, 1967). The wide variation in sedimentary structures and grain size documented for this facies is interpreted as representing paleosols in various stages of development and the different sediment deposits on which soil development took place (e.g., Machette, 1985).

Facies F8

Description. Facies F8 consists of well sorted, mildly bioturbated, medium to coarse sandstone that variably contains scattered fine gravel clasts (Fig. 2H). The sandstone typically displays horizontal stratification, but appears almost massive in some exposures. The predominant fine sediment content of this facies contrasts strongly with the relatively coarse-grained facies that make up most of the alluvium. Facies F8 occurs as lenticular sandstone drapes, found in association with Facies F1 and F2. The facies is typically less than 30 cm thick and laterally continuous for less than 2 m. This facies is not volumetrically significant and is only found in the Portal 1 and 40mBIG measured sections (Figs. 3B, 3C).

Interpretation. Facies F8 is interpreted as representing finer sediment deposited in shallow channels on tops of bars and along the flanks of bars during falling-stage and low-stage flows (e.g., Rust, 1972; Miall, 1977).

Depositional Model and Facies Architecture

Our sedimentologic analysis of the facies of the alluvium exposed in Fortymile Wash shows the bulk of the deposits consists of horizontally stratified conglomerate and sandstone (Facies F1) and massive clast-supported conglomerate (Facies F4) (Figs. 3,4). Interbedded with these two dominant facies are minor lenticular lenses of clast-supported conglomerate (Facies F2), cross-stratified conglomerate (Facies F3), and massive to horizontally stratified sandstone (Facies F8). Facies F1–F4, and F8 are interpreted as the products of deposition within a network of active braided-stream channels and intervening bars. Collectively, the common occurrence of massive and horizontally stratified conglomerate and sandstone; clast-supported and imbricated conglomerate; internal scour surfaces; and lenticular lenses of cross-stratified

conglomerate indicate high-energy stream flow was the dominant depositional process for the alluvium of Fortymile Wash. These types of facies are typical in braided-stream fluvial channels and are the result of deposition and migration of longitudinal bars and shallow channels (see Miall, 1977; Rust, 1978; Collinson, 1986).

We interpret the reddish, well-cemented, massive sandstone with outsized cobble clasts (Facies F7) and the gravel-to-boulder horizons forming calcrete horizons (Facies F6) as the products of paleosol formation. These paleosols developed in areas laterally adjacent to active channels. The presence of paleosols in the alluvium indicates that parts of Fortymile Wash underwent prolonged periods of subaerial exposure, during which the deposited alluvium became bioturbated by plants, and detrital ferromagnesium minerals became oxidized (reddened). The varying degrees of bioturbation and caliche development in the paleosols reflect different lengths of exposure for pedogenesis. Deposits of debris flows or other sediment gravity flows are limited to the one occurrence of Facies F5 in the Portal 1 measured section (Fig. 3B). The lack of debris flow deposits is likely because of the location of studied outcrops along the main trunk channel of Fortymile Wash, as opposed to the margins of Fortymile Wash where relict deposits are present and where modern sediment gravity flow processes are active (Coe et al., 1997; Ressler, 2001).

The facies architecture of two exposures of alluvium in Fortymile Wash is illustrated in Figure 4. Figure 4A shows the alluvium in the Portal 1 outcrop is dominated by the horizontally stratified conglomerate and sandstone of Facies F1. Note that in this outcrop, Facies F1 is internally partitioned by lenticular lenses of clast-supported conglomerate (Facies F2) and cross-stratified conglomerate (Facies F3), but overall, Facies F1 shows a high degree of interconnectedness. Overlying the channel facies in this outcrop is a laterally continuous

paleosol facies (Facies F7). Figure 4B shows the facies architecture from our 40mBIG outcrop and highlights the partitioning of channel facies by laterally continuous paleosol facies. Note that this outcrop can be subdivided into three channel packages separated by paleosol facies. The lower unit consists of horizontally stratified conglomerate and sandstone (Facies F1) with interbedded lenses of clast-supported conglomerate (Facies F2). The middle package consists of clast-supported conglomerate (Facies F1/F4) overlain by a laterally continuous paleosol facies (Facies F7). Above this paleosol is an upper package of clast-supported conglomerate (Facies F4) that is overlain by another laterally extensive paleosol facies (Facies F7). Also note the thin discontinuous calcrete horizons (Facies F6) that are common throughout the upper part of the 40mBIG outcrop.

In summary, the facies architecture of alluvium exposed in Fortymile Wash is characterized by channel facies on the order of 10 m thick, separated by laterally continuous paleosol facies on the order of 1–2 m thick. The channel facies has an overall tabular geometry, but internally exhibits considerable heterogeneity with many laterally discontinuous lenses of conglomerate and sandstone. The facies architecture of the alluvium previously described has been developed based solely on observations of two-dimensional outcrop exposures along the north-south-trending Fortymile Wash. Additional observations regarding the east-west lateral extent and geometries of the different facies in Fortymile Wash are needed to understand three-dimensional facies geometries. Given that the majority of outcrops are oriented parallel to the flow direction of Fortymile Wash, other methods besides direct observation, such as geophysical methods, must be explored for examining the geometry of the different facies in other orientations.

A key question in our analysis of the alluvium in sedimentary basins adjacent to Yucca Mountain is whether the exposures in Fortymile Wash are representative of the alluvium in the saturated alluvial aquifer. Recently, the Nye County Early Warning Drilling Program used a sonic coring method in Well NC–EWDP–19PB to extract intact core of the saturated alluvium to better understand the rock properties of this relatively unstudied interval. The upper 106 m (350 ft) of the borehole was drilled using conventional rotary drilling methods and cased off to provide access for core drilling. The lower section was continuously cored using the sonic coring method in the saturated zone from 106 to 193 m (350 to 634 ft) below ground surface. The sonic core provided excellent recovery of unconsolidated and cemented conglomerate sediments and permitted us to identify bedding and general sedimentary textures, such as grain-size trends.

Inspection of the 19PB core documented two dominant lithofacies. One lithofacies is characterized by 30–50-cm-thick gravel-sand couplets that fine-upward. The second lithofacies is of well-organized, clast-supported conglomerate. The gravel-sand couplets are particularly well developed from 161–185 m (529–606 ft) in the core; the conglomerate lithofacies is well developed at intervals 161–166 m (529–546 ft) and 151–157 m (495–516 ft). These two most common lithofacies in the core also are the two most common lithofacies (F1 and F4) documented in our measured sections from the exposures in Fortymile Wash. The core also contains medium-grained sandstone intervals, often with a reddish color, that appear quite similar to the paleosol lithofacies (F7) described from our measured sections in Fortymile Wash. A representative example of this lithofacies is found in the core at 134–137 m (441–448 ft). We interpreted the consistency between the measured section and subsurface core data as evidence the Fortymile Wash outcrops are representative of alluvium in the saturated aquifer.

Hydraulic Properties

Studies of the porosity and permeability of Quaternary alluvium in sedimentary basins of the southwestern United States are few (e.g., Bedinger et al., 1989). The extremely coarse grain sizes and the often unconsolidated nature of most lithologies in the alluvium make it difficult to use traditional methods, such as core analysis, to determine aquifer properties. Because of these inherent problems, we calculated aquifer properties using several different techniques: (1) analyses of samples that are disaggregated in the field and then repacked for laboratory analysis (referred to as disturbed samples in the text), (2) analyses of oriented samples collected as large intact blocks in the field and measured in the laboratory (referred to as undisturbed samples in the text), and (3) estimates based on grain-size analyses of alluvium samples. In this section, we present results of measurements from each technique; compare the results of the different techniques; and evaluate our results against previous published techniques that use empirical relations based on grain-size to determine hydraulic conductivity (Shepherd, 1989; Vukovic and Soro, 1992). All hydraulic conductivity values discussed in the text for alluvium of Fortymile Wash are for saturated conditions.

Disturbed Sample Hydraulic Conductivity

Representative disturbed sediment samples were collected from each facies and, in most cases, collected from multiple exposures of each facies. The disturbed sediment samples were repacked to an estimated *in-situ* bulk density in the laboratory to create test specimens for constant head permeameter tests. The *in-situ* bulk density for a disturbed sediment sample was estimated from the mass of sediment removed from the outcrop and the volume of the space created by removal of this sediment. Three different test specimens were created from each

sediment sample and each tested to examine the consistency of the hydraulic conductivity test results (Table 2). The hydraulic conductivity tests were conducted following the procedure described by Kresic (1997). Details regarding preparation and completion of the disturbed sediment hydraulic conductivity tests are provided in Ressler (2001).

Numerous empirical relations (Shepherd, 1989; Vukovic and Soro, 1992) also were used to determine hydraulic conductivity from the results of grain-size analyses conducted for disturbed sediment samples. These empirical hydraulic conductivity estimates tested whether reasonable hydraulic conductivity values for the Fortymile Wash alluvium could be obtained from empirical relations. Several empirical relations presented by Shepherd (1989) that were developed from grain-size data sets of river alluvium were chosen for comparison (Table 3). Additional empirical relations from Vukovic and Soro (1992) also were chosen for comparison (Table 3). Unlike the empirical relations presented by Shepherd (1989), the empirical relations provided by Vukovic and Soro (1992) explicitly relate total porosity to hydraulic conductivity, in addition to grain-size characteristics. Where applicable, the empirical relations provided by Shepherd (1989) and Vukovic and Soro (1992) were used to estimate hydraulic conductivity from the grain-size analyses of alluvium from Fortymile Wash (Table 3).

Undisturbed Sample Hydraulic Conductivity

Representative, undisturbed sediment samples were obtained from all facies, except for the most coarse-grained facies (those containing cobbles and boulders) where the extreme grain size and poor consolidation made undisturbed sampling nearly impossible and representative sampling impractical. It should be noted that even in facies where intact blocks were obtained, the collected samples are biased toward the more easily collected, better indurated portions of the facies. Attempts were made to collect samples from each of the facies in several localities in

Fortymile Wash; however, due to difficulty removing intact samples, not all of the facies were equally represented in the collected samples.

Intact blocks of alluvium were excavated from outcrop via rock hammer and chisel. Intact and oriented sediment test specimens were obtained from the undisturbed blocks for laboratory determination of hydraulic conductivity and porosity. Hydraulic conductivity tests were conducted following the procedure described by Kresic (1997). Details regarding the preparation of the undisturbed sediment test specimens and the completion of the hydraulic conductivity tests are provided in Ressler (2001). Results from this part of the analysis are shown in Table 2.

Porosity

Estimates of total porosity were developed from the undisturbed sediment test specimens and from the results of the grain-size analyses of the disturbed sediment samples. Porosity determination tests of the undisturbed sediment test specimens were conducted following a procedure modified from the water desorption method of Danielson and Sutherland (1986).

Estimates of total porosity were developed from grain-size data using an empirical relation based on the coefficient of uniformity provided by Vukovic and Soro (1992). Results from this part of the analysis are shown in Table 2.

Grain-Size Analyses

The grain-size analyses conducted for disturbed sediment samples of the alluvium were completed following the methodology prescribed by American Society for Testing and Materials (ASTM) standard D 422-63 (2000). ASTME–11 sieve numbers 1", 5/8", 5/16", 4, 10, 20, 40, 60, 140, and 200 were used for the sieve analyses, and an ASTM 152H hydrometer was used for the hydrometer analyses of sediment finer than the number 200 sieve.

Discussion of Hydraulic Properties

Laboratory-derived porosity estimates show a range in total porosity of 0.21–0.36 (Fig. 5A), with the coarser grained samples (Facies F1 and F2, Fig. 5A) having lower porosities (0.21–0.29) than the finer grained samples (Facies F7 and F8, Fig. 5A) with porosities 0.29–0.36. Grain-size-derived porosity estimates show a slightly higher range of porosity, ranging from 0.26 to 0.28 for the coarser grained samples and from 0.38 to 0.42 for the finer grained samples (Fig. 5A). The empirical grain-size-porosity relation from Vukovic and Soro (1992) performed remarkably well in approximating the laboratory-derived porosities (Table 2, Fig. 5). The empirical relation seems to approximate more precisely the laboratory-derived porosity estimates for the coarser grained samples than for the finer grained samples. This likely reflects the fact that the finer grained sediments in the Fortymile Wash alluvium are often more strongly cemented than are the coarser grained sediments, while the empirical grain-size-porosity relation is based on grain-size data from unconsolidated sand and gravel.

Results of the disturbed sediment hydraulic conductivity tests indicate that hydraulic conductivity varies over three orders of magnitude, ranging from 10^{-3} to 10^{-6} cm/s (Fig. 5B). The most permeable sample (40mDS1), collected from a layer of open-framework conglomerate

within Facies F1, had hydraulic conductivities ranging from 2.21×10^{-3} to 2.30×10^{-3} cm/s (Table 2). Several other samples from Facies F1 consisting of a mix of sand and gravel of slightly different grain sizes were found to have hydraulic conductivities within the range of 10^{-4} cm/s. The least permeable samples were from Facies F8 (40mDS3) and Facies F7 (40mDS7 and 40mDS12), with hydraulic conductivities in the range 10^{-5} cm/s to 10^{-6} cm/s (Table 2, Fig. 5B). These disturbed sediment hydraulic conductivity tests were conducted for columns of alluvium repacked in the laboratory; thus, the grain arrangement, cementation, and density differ from the *in-situ* state of the alluvium.

To represent the *in-situ* state of the alluvium, undisturbed blocks of the alluvium also were collected from each facies. The undisturbed sediment hydraulic conductivity tests indicate that Facies F1 is the most permeable facies, with hydraulic conductivities ranging from 3.0×10^{-4} to 3.9×10^{-3} cm/s (Table 2, Fig. 5B). The open-framework conglomerate in Facies F1 is not represented in the undisturbed sediment samples because an intact sample could not be collected because of its coarse grain size and poor induration. The open-framework conglomerate in Facies F1 is expected to be more permeable than the undisturbed sediment samples collected, thus, the range in hydraulic conductivity within Facies F1 is expected to exceed that shown by the undisturbed sediment hydraulic conductivity data. The least permeable undisturbed sediment samples were from Facies F2, F7, and F8. The sand matrix from Facies F2 had a hydraulic conductivity of 9.0×10^{-5} cm/s, Facies F7 had hydraulic conductivities ranging from 2.0×10^{-4} to 2.5×10^{-3} cm/s, and Facies F8 had hydraulic conductivities ranging from 4.0×10^{-4} to 2.6×10^{-3} cm/s (Table 2, Fig. 5B). Results of the undisturbed sediment hydraulic conductivity tests indicate a similar range in hydraulic conductivity between facies compared to the disturbed sediment hydraulic conductivity estimates. The undisturbed sediment hydraulic conductivity

estimates, however, appear to be systematically higher than the disturbed sediment hydraulic conductivity estimates (Fig. 5B). This observation likely reflects grain rearrangement and overpacking of the alluvium samples during preparation of the disturbed sediment test specimens. There also is a larger difference between the undisturbed sediment and disturbed sediment hydraulic conductivity estimates for the samples from the finer grained facies (Facies F7 and F8) than for the coarser grained facies (Facies F1). A larger number of undisturbed sediment and disturbed sediment samples were collected from Facies F1 than from Facies F7 or F8. The lack of overlap in undisturbed sediment and disturbed sediment hydraulic conductivity estimates for Facies F7 and F8, therefore, may be due, in part, to the fewer number of samples collected and tested.

Compared to the undisturbed sediment hydraulic conductivity estimates, the empirical hydraulic conductivities developed using relations from Shepherd (1989) show a similar relative variation in hydraulic conductivity between the different facies but greatly overestimate the undisturbed sediment hydraulic conductivities of all samples (Table 3, Fig. 5C). The large difference (≥350%) between the undisturbed sediment hydraulic conductivities and the empirical hydraulic conductivities most likely results from the lack of a consolidation or cementation factor in the relations from Shepherd (1989).

The empirical relations from Vukovic and Soro (1992) explicitly relate hydraulic conductivity to various grain-size parameters, total porosity, and properties of the fluid of interest. The empirical relations from Vukovic and Soro (1992) produce hydraulic conductivities that exceed the undisturbed sediment hydraulic conductivities for all but a few of the alluvium samples; however, these empirical relations produce hydraulic conductivities that more closely approximate the undisturbed sediment hydraulic conductivities than do the

relations from Shepherd (1989) (Fig. 5D). The Krüger equation and the Slichter equation were the best performing empirical relations, producing hydraulic conductivity estimates with less than one order of magnitude deviation from the undisturbed sediment hydraulic conductivities (Ressler, 2001). According to the limits provided by Vukovic and Soro (1992), the Krüger equation is applicable only for the coarser grained alluvium samples; but even outside the recommended domain of applicability, this equation provides the closest approximation to the undisturbed sediment hydraulic conductivity estimates (Table 3). The empirical hydraulic conductivity estimates using the grain-size-derived porosity estimates show a slightly larger degree of deviation from the undisturbed sediment hydraulic conductivities than do the empirical hydraulic conductivity estimates using the laboratory-derived porosity estimates (Figs. 5E, 5F). This result is not unexpected, because the laboratory-derived porosity estimates are more representative approximations of the in-situ porosity of the alluvium than are the grain-size-derived porosity estimates.

Summary of Hydraulic Properties

The aquifer properties determined in this study identify the gross variations of hydraulic properties of different facies within the alluvium of Fortymile Wash and provide insight into the limitations of various techniques used for determination of porosity and hydraulic conductivity in alluvium. Estimates of total porosity in the alluvium of Fortymile Wash range from 0.21 to 0.42, and hydraulic conductivity varies at least three orders of magnitude between the different facies. Overall, the conglomerate-dominated facies have lower porosities and higher hydraulic conductivities than do the sandstone-dominated facies.

Results of the laboratory hydraulic conductivity tests for the undisturbed sediment samples are considered the most representative approximation of the *in-situ* hydraulic conductivity of the alluvium. The hydraulic conductivity test specimens created from repacked alluvium likely underestimate *in-situ* hydraulic conductivity. For the most part, the various empirical grain-size-hydraulic conductivity relations overestimate the laboratory-measured hydraulic conductivity of the undisturbed sediment test specimens. However, the empirical grain-size-hydraulic conductivity relations involving multiple grain-size parameters and porosity (Vukovic and Soro, 1992) better approximated the undisturbed sediment hydraulic conductivity estimates than did the relations that involved only grain-size parameters (Shepherd, 1989). In particular, the Krüger and Slichter empirical relations (Vukovic and Soro, 1992) were capable of approximating the undisturbed sediment hydraulic conductivity within one order of magnitude. Based on our results, these two relations show promise for estimating bulk hydraulic conductivity from grain-size data in future studies of alluvial aquifers. Similarly, the empirical relation from Vukovic and Soro (1992) relating porosity to the uniformity coefficient of the sediment performed quite well in approximating laboratory-determined porosities of undisturbed samples of alluvium. The empirical grain-size-porosity relation was developed for unconsolidated sediments; thus, the relation performs better for the coarser grained alluvium that tends to be less cemented than the finer grained alluvium.

Implications for Groundwater Flow

Our estimates of porosity and hydraulic conductivity, combined with facies architecture data, provide a framework to understand the spatial heterogeneity and distribution of aquifer properties. Aquifer characterization of alluvium in Fortymile Wash provides the best available

analog of the alluvial aquifer down gradient from the potential nuclear waste repository at Yucca Mountain. As discussed in an earlier section, the facies architecture of the alluvium is characterized by channel facies (Facies F1, F2, F3, F4, and F8) that are on the order of 10 m thick and are separated by fairly laterally-continuous, paleosol facies (Facies F6 and F7) that are on the order of 1–2 m thick. Our hydraulic data show that the conglomerate-dominated channel facies have lower porosities and higher hydraulic conductivities than the sandstone-dominated paleosol facies. The integration of the facies and hydraulic properties data suggests that the interlayering of thicker, more permeable channel facies with thin, less permeable paleosol facies may stratify and compartmentalize groundwater flow through the alluvial aquifer. For example, the relative low hydraulic conductivity of paleosol Facies F7 in conjunction with its lateral continuity suggests that this facies may stratify vertical and horizontal groundwater movement. Results of previous investigations of Fortymile Wash alluvium support our conclusion. During infiltration investigations conducted near our 40mBIG outcrop (Fig. 1B), for example, Guertal et al. (1994) found that the downward movement of water was strongly retarded by petrocalcic (caliche or calcrete) horizons and that there was substantial horizontal movement of water atop the caliche horizons. These petrocalcic horizons, as described by Guertal et al. (1994), include pedogenic calcrete layers and paleosols, which are defined as Facies F6 and F7 in our study. Saturated conditions are unlikely to preserve the calcrete layers. However, we observe medium to coarse grain sands, similar to those in Facies F7 in the Nye County sonic core 19PB from 134 to 137 m (440 to 450 ft.) Our interpretations are also consistent with other studies of alluvial-fan and fluvial aquifers that suggest that paleosols act as baffles to subsurface fluid flow (e.g., Galloway and Sharp, 1998a, 1998b; Weissmann and Fogg, 1999). In general, our findings suggest that low-permeability paleosol facies in the alluvial aquifer down gradient of Yucca

Mountain may enhance stratification of hydraulic conductivity and impart a horizontal anisotropy to groundwater flow.

In addition to the stratification of hydraulic conductivity, the open-framework conglomerates could serve as conduits for ground water flow within the channel facies in Facies F1. The most permeable disturbed sediment sample measured in our analysis (40mDS1 in Table 1) was from the open-framework conglomerate of Facies F1. In many cases, this conglomerate is significantly coarser in outcrop than represented by the collected samples; thus, the maximum hydraulic conductivity will probably surpass the range shown by the current data. The open-framework conglomerate within Facies F1 is likely to have the highest hydraulic conductivity within the alluvial aquifer. Because it can accommodate larger groundwater flows, the interconnectedness of the open-framework conglomerate within Facies F1 will be important for assessing the internal heterogeneity of transmissive zones (i.e., channel facies) and the larger-scale hydraulic conductivity in the alluvial aquifer. This assertion is supported by numerical modeling results on glacial outwash deposits that show there are preferential groundwater flow paths even within deposits of highly permeable gravel (e.g., Aiken and Mickelson, 1995).

Additional predictions regarding hydraulic conductivity variations in the alluvial aquifer are based upon the braided stream depositional model proposed for outcrops of Fortymile Wash. In this type of depositional environment, the active channel consists of braid channels and intervening bars. The active channel zone was the site for the accumulation of Facies F1, F2, F3, F4, and F8. Laterally bounding the active channel were areas bypassed by active sedimentation (i.e., floodplains), which are reflected in the stratigraphic record by paleosol facies (Facies F7 and F6). Accordingly, the continuity and orientation of the more permeable channel facies are expected to be greater parallel to rather than perpendicular to the modern channel direction of

Fortymile Wash. This relationship would produce a bulk horizontal anisotropy in the hydraulic properties of the alluvial aquifer.

CONCLUSIONS

Well exposed outcrops of alluvium in Fortymile Wash provide a unique analog of the alluvial aquifer down gradient from the proposed high-level nuclear waste repository at Yucca Mountain. Eight diagnostic sedimentary facies are identifiable in the alluvium of Fortymile Wash. The facies are interpreted as the products of fluvial deposition within a network of active braid channels and intervening bars. Laterally bounding the active channel zones are areas bypassed by active sedimentation (i.e., floodplains), reflected in the stratigraphic record by paleosols. The facies architecture of the alluvium of Fortymile Wash is characterized by channel facies that are on the order of 10 m thick and are separated by laterally continuous, well-cemented, paleosol facies that are on the order of 1–2 m thick. A recent sonic core of the alluvium in Nye County well NC-EWDP-19PB confirms that the facies described from outcrop also occur in the subsurface, within the saturated alluvial aquifer down gradient from Yucca Mountain.

Hydraulic estimates for the different facies were developed from laboratory permeameter tests and from empirical relations based on the results of grain-size analyses. These data provide a framework to understand the distribution of aquifer properties. Estimates of total porosity range from 0.21 to 0.42, and hydraulic conductivity varies over at least three orders of magnitude (10^{-3} to 10^{-6} cm/sec) between the different facies. The least permeable facies in the alluvium are the paleosol facies, whereas the most permeable facies are the channel facies.

Our new facies and hydraulic properties data suggest to us that the interlayering of more permeable channel facies with less permeable paleosol facies may result in vertical compartmentalization of groundwater flow through the alluvial aquifer. Our analysis also suggests that the highest hydraulic conductivity in the alluvial aquifer will be associated with the open-framework conglomerate within the channel facies.

REFERENCES

Aiken, J.S., and Mickelson, D.M., 1995, Three-dimensional characterization of hydraulic properties of a coarse glacial outwash deposit: Madison, Groundwater Research Report WRC GRR 95-01, University of Wisconsin-Madison.

Allen, J.R.L., 1986, Pedogenic calcretes in the Old Red Sandstone facies (Late Silurian-Early Carboniferous) of the Anglo-Welsh area, southern Britain, *in* Wright, V.P., ed., Paleosols-their recognition and interpretation, p. 58-86.

American Society for Testing and Materials, 2000, Standard test method for particle-size analysis of soils (D 422-63): Annual Book of ASTM Standards 04.08.

Bechtel SAIC Company, LLC, 2003a, Technical Basis Document No. 11: Saturated Zone Flow and Transport, Rev. 2, Las Vegas, Nevada: Bechtel SAIC Company, LLC.

Bechtel SAIC Company, LLC, 2003b, Saturated Zone In-Situ Testing, ANL–NBS–HS–000039, REV 00, Las Vegas, Nevada: Bechtel SAIC Company, LLC.

Bedinger, M.S., Langer, W.H., and Reed, J.E., 1989, Hydraulic properties of rocks in the Basin and Range Province, *in* Bedinger, M.S., Sargent, K.A., Langer, W.H., Sherman, F.B., Reed, J.E., and Brady, B.T., eds., Studies of geology and hydrology in the Basin and Range Province, southwestern United States, for isolation of high-level radioactive waste-basis of characterization and evaluation: U.S. Geological Survey Professional Paper 1370-A, p. 16–18.

Blair, T.C., 1987, Sedimentary processes, vertical stratification sequences, and geomorphology of the Roaring River alluvial fan, Rocky Mountain National Park, Colorado: Journal of Sedimentary Petrology, v. 57, p. 1–18.

Blair, T.C., and McPherson, J.G., 1994, Alluvial fans and their natural distinction from rivers based on morphology, hydraulic processes, sedimentary processes, and facies assemblages: Journal of Sedimentary Research, v. A64, p. 450–489.

Coe, J.A., Glancy, P.A., and Whitney, J.W., 1997, Volumetric analysis and hydrologic characterization of a modern debris flow near Yucca Mountain, Nevada: Geomorphology, v. 20, p. 11–28.

Collinson, J.D., 1986, Alluvial sediments, *in* Reading, H.G., ed., Sedimentary environments and facies: Oxford, Blackwell, p. 20–62.

Danielson, R.E. and Sutherland, P.L., 1986, Porosity, *in* Klute, A., ed., Methods of soil analysis: Part 1-Physical and mineralogical methods: Agronomy Monograph 9, American Society of Agronomy, Inc., p. 443–461.

Folk, R.L., and Ward, W.C., 1957, Brazos River bar: A study in the significance of grain size parameters: Journal of Sedimentary Petrology, v. 27, p. 3–26.

Galloway, W.E., and Sharp, J.M., Jr., 1998a, Characterizing aquifer heterogeneity within terrigenous clastic depositional system, *in* Fraser, G.S., and Davis, J.M., eds., Hydrogeologic models of sedimentary aquifers: Society for Sedimentary Geology-Concepts in Hydrogeology and Environmental Geology, No. 1, p. 85–90.

Galloway, W.E., and Sharp, J.M., Jr., 1998b, Hydrogeology and characterization of fluvial aquifer systems, *in* Fraser, G.S., and Davis, J.M., eds., Hydrogeologic models of sedimentary aquifers: Society for Sedimentary Geology-Concepts in Hydrogeology and Environmental Geology, No. 1, p. 91–106.

Gile, L.H., and Hawley, J.W., 1966, Periodic sedimentation and soil formation on an alluvial-fan piedmont in southern New Mexico: Soil Science Society of America Proceedings, v. 30, p. 261–268.

Glancy, P.C., and Beck, D.A., 1998, Modern flooding and runoff of the Amargosa River, Nevada, California, emphasizing contributions of Fortymile Wash. Quaternary Geology of the Yucca Mountain Area, Southern Nevada: Field Trip Guide, Friends of Pleistocene, Pacific Cell, p. 51–62.

Guertal, W.R., Flint, A.L., Hofmann, L.L., and Hudson, D.B., 1994, Characterization of a desert soil sequence at Yucca Mountain, NV: High Level Radioactive Waste Management 4, p. 2,755–2,763.

Holliday, V.T., 1989, The Blackwater Draw Formation (Quaternary): A 1.4-plus-m.y. record of eolian sedimentation and soil formation on the southern High Plains: Geological Society of America, v. 101, p. 1598–1607.

Kresic, N. 1997, Quantitative solutions in hydrogeology and groundwater modeling: CRC Press LLC.

Lattman, L. H., 1973, Calcium carbonate cementation of alluvial fans in southern Nevada: Geological Society of America Bulletin, v. 84, p. 3013–3028.

Lundstrom, S.C., McDaniel, S.M., Guertal, W., Nash, M.H., Wesling, J.R., Cidziel, J., Cox, S., and Coe, J., 1995, Characteristics and development of alluvial soils of the Yucca Mountain Area, southern Nevada: Milestone Report 3CCH510M.

Lundstrom, S.C., Paces, J.B., and Mahan, S.A., 1998, Late Quaternary history of Fortymile Wash in the area near the H-road crossing. Quaternary geology of the Yucca Mountain Area, southern Nevada: Field Trip Guide, Friends of Pleistocene, Pacific Cell, p. 63–76.

Machette, M.N., 1985, Calcic soils of the southwestern United States, *in* Weide, D.L., eds., Soils and Quaternary geology of the southwestern United States: Geological Society of America Special Paper 203, p. 1–21.

Mack, G.H., James, W.C., and Monger, H.C., 1993, Classification of paleosols: Geological Society of America Bulletin, v. 105, p. 129–136.

Miall, A.D., 1977, A review of the braided-river depositional environment: Earth Science Review, v. 13, p. 1–62.

Mohanty, S., and McCartin, T.J., 1998, Total-system Performance Assessment (TPA) Version 3.2 Code: Module descriptions and user's guide: Center for Nuclear Waste Regulatory Analyses.

Nemec, W., and Steel, R.J., 1984, Alluvial and coastal conglomerates: their significant features and some comments on gravelly mass-flow deposits, *in* Koster, E.H., and Steel, R.J., eds., Sedimentology of gravels and conglomerates: Canadian Society of Petroleum Geologists Memoir 10, p. 1–31.

Nye County, 1999, Nye County early warning drilling program: Phase I-FY1999 Data Package, Pahrump, NV: Nye County Nuclear Waste Repository Project Office.

Oatfield, W.J., and Czarnecki, J.B., 1989, Hydrogeologic inferences from driller's logs and from gravity and resistivity surveys in the Amargosa Desert, southern Nevada: U.S. Geological Survey Open-File Report 89–234.

Paces, J.B., Menges, C.M., Widmann, B., Wesling, J.R., Bush, C.A., Futa, K., Millard, H.T., Maat, P.B., and Whitney, J.W., 1994, Preliminary U-series disequilibrium and thermoluminescence ages of surficial deposits and paleosols associated with Quaternary faults, eastern Yucca Mountain: Proceedings of the Fifth Annual International

Conference on High-level Radioactive Waste Management, Las Vegas, Nevada, La Grange Park, IL, American Nuclear Society, p. 2,391–2,401.

Questa Engineering Corp, 2001, Analysis of Pump-Spinner Test and 48-Hour Pump Test in Well NC–EWDP–19D, Near Yucca Mountain, Nevada, NWRPO–2001–03, Pahrump, Nevada: Nye County Department of Natural Resources and Federal Facilities, Nuclear Waste Repository Project Office.

Reimus, P. and Umari, M.J., 2002, Test Plan for Alluvial Testing Complex—Single-Well, Multi-Well, and Laboratory Studies, Letter Report SITP–02–SZ–003, North Las Vegas, Nevada: DOE, Office of Civilian Radioactive Waste Management, Yucca Mountain Site Characterization Office.

Ressler, T.R., 2001, Preliminary characterization of the valley-fill aquifer in Fortymile Wash, southwestern Nevada [Master's thesis] Austin, The University of Texas at Austin.

Retallack, G.J., 1983, Late Eocene and Oligocene paleosols from Badlands National Park, South Dakota: Geological Society of America Special Paper 193, 82 p.

Retallack, G.J., 1990, Soils of the past: An introduction to paleopedology: Boston, Unwin Hyman, 520 p.

Ridgway, K.D., and DeCelles, P.G., 1993, Stream-dominated alluvial fan and lacustrine depositional systems in Cenozoic strike-slip basins, Denali fault system, Yukon Territory, Canada: Sedimentology, v. 40, p. 645–666.

Ridgway, K.D., Trop, J.M., and Sweet, A.R., 1997, Thrust-top basin formation along a suture zone, Cantwell basin, Alaska Range: Implications for development of the Denali fault system: Geological Society of America Bulletin, v. 109, p. 505–523.

Robinson, J.H., 1984, Ground-water level data and preliminary potentiometric-surface maps: Yucca Mountain and Vicinity, Nye County, Nevada: U.S. Geological Survey Water-Resources Investigations Report 84-4197.

Rust, B.R., 1972, Structure and process in a braided river: Sedimentology, v. 18, p. 221–245.

Rust, B.R., 1978, A classification of alluvial channel systems: *in* Fluvial Sedimentology, Maill, A.D., ed., Can Soc Petrol Geol Mem 5, p. 187–198.

Shepherd, R.G., 1989, Correlations of permeability and grain size: Ground Water, v. 27, p. 633–638.

Siegenthaler, C., and Huggenberger, P., 1993, Pleistocene Rhine gravel: Deposits of a braided river system with dominant pool preservation, *in* Best, J.L. and Bristow, C.S., eds., Braided rivers: Geological Society Special Publication 75, The Geological Society, p. 147–162.

Smith, N.D., 1970, The braided stream depositional environment: Comparison of the Platte River with some Silurian clastic rocks, north-central Appalachians: Geological Society of America Bulletin, v. 81, p. 2993–3014.

Smith, N.D., 1974, Sedimentology and bar formation in the upper Kicking Horse River, a braided outwash stream: Journal of Geology, v. 82, p. 205–223.

Snyder, B.B., and Carr, W.J., 1982, Preliminary results of gravity investigations at Yucca Mountain and vicinity, southern Nye County, Nevada: U.S. Geological Survey Open-File Report 82-701.

Todd, S.P., 1996, Process deduction from fluvial sedimentary structures, in Carling, P.A., and Dawson, M.R., eds., Advances in fluvial dynamics and stratigraphy: Chichester, John Wiley & Sons, Inc.

VanArsdale, R., 1982, Influence of calcrete on the geometry of arroyos near Buckeye, Arizona: Geological Society of America Bulletin, v. 93, p. 20–26.

Vukovic, M., and Soro, A., 1992, Determination of hydraulic conductivity of porous media from grain-size composition: Water Resources Publications.

Walker, G.E., and Eakin, T.E., 1963, Ground-water resources-reconnaissance series report 14, Geology and groundwater of Amargosa Desert, Nevada, California: U.S. Geological Survey, Nevada Department of Conservation and Natural Resources.

Walker, T.R., 1967, Formation of red beds in ancient and modern deserts: Geological Society of America Bulletin, v. 8, p. 353–368.

Weissmann, G.S., and Fogg, G.E., 1999, Multi-scale alluvial fan heterogeneity modeled with transition probability geostatistics in a sequence stratigraphic framework: Journal of Hydrology, v. 226, p. 48–65.

Winterle, J., 2003, Evaluation of Alternative Concepts for Saturated Zone Flow: Effects of Recharge and Water Table Rise on Flow Paths and Travel Times at Yucca Mountain, San Antonio, Texas: CNWRA.

Winterle, J., and Farrell, D.A., 2002, Hydrogeologic Properties of the Alluvial Basin Beneath Fortymile Wash and Northern Amargosa Valley, Southern Nevada, San Antonio, Texas: CNWRA.

FIGURE CAPTIONS

Figure 1 **(A)** Regional map of the Yucca Mountain area in southwestern Nevada and southeastern California. Black triangles mark locations of measured stratigraphic sections in Fortymile Wash discussed in text. Blue dots mark locations of wells drilled as part of the Nye County Early Warning Drilling Program. Well names are labeled in black next to each location. NTS = Nevada Test Site. **(B)** Site map of Yucca Mountain and Fortymile Wash. Abbreviations mark locations of measured stratigraphic sections discussed in text.

Figure 2 Photographs of common facies in alluvium of Fortymile Wash. **(A)** Facies F1: horizontally stratified conglomerate and sandstone forming gravel-sand couplets. Red arrows mark the base and top of a single gravel-sand couplet. Shows a close-up of an open framework conglomerate. **(B)** Facies F2: clast-supported, organized pebble to boulder conglomerate with a matrix of medium to coarse sandstone. **(C)** Facies F3: lenticular unit of cross-stratified conglomerate within horizontally stratified conglomerate of Facies F1. Inset highlights the cross-stratification within the lenticular unit. **(D)** Facies F4: poorly sorted conglomerate displaying crude horizontal stratification. Red arrows to the left highlight crude layering of coarser and finer grain sizes. The thin white arrow to the right highlights a small lens of fine conglomerate and sandstone within the facies. **(E)** Facies F5: clast-supported, disorganized conglomerate consisting of dominantly monolithologic angular gravel to boulders with a matrix of medium to coarse sand. **(F)** Facies F6: layers of gravelly calcrete developed beneath a highly bioturbated paleosol consisting of coarse sandstone with scattered gravel and cobbles to boulders. Red arrows highlight individual calcrete horizons. **(G)** Facies F7: lenticular shaped sandstone body consisting of strongly cemented, mildly bioturbated medium to coarse sand with

a distinctive reddish color. **(H)** Facies F8: lenticular sandstone drape consisting of well sorted, medium to coarse sand.

Figure 3 Stratigraphic sections measured from the investigated outcrops in the entrenched channel of Fortymile Wash. See Figure 1B for locations.

Figure 4 Photographs of outcrops and facies architecture maps showing distribution and 2-D geometry of facies in alluvium of Fortymile Wash. See Figure 1B for location of outcrops. **(A)** The spatial distribution of channel facies F1, F2, and F3 is particularly well exposed at the Portal 1 outcrop. Note the dominance and interconnectedness of horizontally stratified conglomerate and sandstone of Facies F1 in this outcrop. **(B)** The 40mBIG outcrop provides an example of the partitioning of channel facies by laterally continuous paleosol facies.

Figure 5 **(A)** A graphical comparison of the laboratory-derived porosity (LP) and grain size-derived porosity (GSP) estimates. **(B)** A graphical comparison of the hydraulic conductivity (K_{sat}) estimates obtained from disturbed sediment (DS) and undisturbed sediment (US) samples collected from alluvium of Fortymile Wash. **(C)** A graphical comparison of the undisturbed sediment hydraulic conductivity (US-K_{sat}) to the hydraulic conductivities developed using the empirical relations from Shepherd (1989). **(D)** A graphical comparison of the undisturbed sediment hydraulic conductivity (US-K_{sat}) to the hydraulic conductivities developed using the empirical relations from Vukovic and Soro (1992). **(E)** A plot of the percent deviation between the undisturbed sediment hydraulic conductivity (US-K_{sat}) and the empirically derived (Vukovic and Soro, 1992) hydraulic conductivities using the grain size-derived porosity (GSP) estimates.

(F) A plot of the percent deviation between the undisturbed sediment hydraulic conductivity (US-K_{sat}) and the empirically derived (Vukovic and Soro, 1992) hydraulic conductivities using the laboratory-derived porosity (LP) estimates.

Table 1. Sedimentary and hydraulic characteristics of the facies delineated within the alluvium of Fortymile Wash. The representative hydraulic properties were derived from an evaluation of the laboratory analyses completed the alluvium samples (the results for individual samples are provided in Tables 2 and 3). For Facies F3, F5, and F6 where alluvium samples were not collected, the representative hydraulic properties are estimated based on sedimentary characteristics in relation to other facies for which alluvium samples were collected.

Facies	Sedimentary Features	Observable Geometries	Interpreted Depositional Environment	Representative	
				Porosity	Hydraulic Conductivity
F1 Figure 2A	• clast-supported, imbrication • sand to cobble • primarily horizontally stratified gravel and sand (gravel-sand couplets); minor low angle planar stratification • coarse component of gravel-sand couplets may have bimodal sediment content; open framework gravels variably contained within couplets	• most common and volumetrically significant facies • gravel couplets 10–50 cm thick	Longitudinal bar deposits	0.27	1×10^{-3} cm/s
F2 Figure 2B	• clast-supported • bimodal grain size consisting of cobbles to boulders and medium to coarse sand	• occurs as lenses within Facies F1 • lenticular for lengths of 10–50 m; 10–50 cm thick; coarser units tend to be thicker	Channel deposits between longitudinal bars	0.29	9×10^{-5} cm/s
F3 Figure 2C	• clast-supported • gravel to cobble • lens-shaped units of cross-stratified gravel; internal stratification varies from base parallel stratification to cross-stratification that is planar or tangential to the base	• occurs as lenses within horizontally stratified gravel • 5–15 m in length; 2 m in thickness	Pool scours at convergence of two braid channels	Greater than Facies F1 (>0.27)	Greater than Facies F1 ($>1\times10^{-3}$ cm/s)
F4 Figure 2D	• clast-supported; poorly sorted, poorly organized; imbrication • sand to boulders, coarse gravel to cobbles predominating • crude stratification to massive • crude gravel couplets • variably contains small lenses of sand • cross-stratified gravel and sand commonly present at top of facies	• gravel couplets are 40–50 cm thick • lenses of sand < 30 cm thick • facies are 2–3 m thick	Deposits of turbulent flood flows	0.27	5×10^{-4} cm/s
F5 Figure 2E	• clast-supported to matrix-supported; disorganized • angular clasts; predominant monolithologic clast content • distinct bimodal sediment content consisting of coarse gravel to boulders and medium to coarse sand	• laterally extensive for 10–15 m; variable in thickness, but < 1 m [Note: based only on a single exposure] This facies is expected to be volumetrically larger in proximity to the mountain slopes rimming Fortymile Wash	Sediment gravity flow; most likely debris flow or rock fall	Similar to Facies F2 (0.29)	Similar to Facies F2 (9×10^{-5} cm/s)
F6 Figure 2F	• gravel to boulders • calcrete horizons	• 5–30 cm in thickness; laterally continuous for 100s of meters, though facies may be locally discontinuous	Pedogenic carbonate associated with paleosols	Less than Facies F7 (<0.34)	Less than Facies F7 ($<4\times10^{-4}$ cm/s)
F7 Figure 2F Figure 2G	• matrix-supported, in some instances nearing clast-supported; mild to heavy bioturbation common • medium to coarse sand, with varying concentrations of gravel to cobbles • distinctive reddish coloration and strong caliche development • internal structure complex	• thickness ranges from 0.5 to 2 m; laterally extensive for 10–100s of meters	Paleosols	0.34	4×10^{-4} cm/s
F8 Figure 2H	• horizontal stratification to massive • dominantly well-sorted, medium to coarse sand; some scattered fine gravel clasts • mild bioturbation in some exposures	• commonly found in association with bimodal gravel units (Facies F2 or Facies F1) • < 30 cm thick; laterally continuous < 2 m	Concentrations of finer sediment deposited during waning flow	0.32	6×10^{-4} cm/s

Table 2. Laboratory-derived porosity (LP), grain size-derived porosity (GSP), and hydraulic conductivity (K_{sat}) estimates for undisturbed samples (US) and disturbed samples (DS) of alluvium from Fortymile Wash. The hydraulic conductivity (K_{sat}) provided in this table is the hydraulic conductivity derived from laboratory permeameter analysis of an undisturbed sample (US) or of a repacked test specimen. The standard deviation presented in this table was calculated from the test runs completed on a given test specimen and is presented only as an indicator of the range in K_{sat} between the test runs completed on the given test specimen.

Facies	US Sample	LP	DS Sample	GSP	K_{sat} (cm/s)	Standard Deviation	Sample Collection Location and Sediment Description
F1	US17-P1 US17-P2	0.35 0.28	DS17	0.38	2.8×10^{-3} 3.9×10^{-3}	$\pm 4.3\times10^{-4}$ $\pm 5.1\times10^{-4}$	40mMED. Sandy component of Facies F1. Notable layering of coarser and finer grain sizes. Sample breaks along weaker cemented layers.
	No sample		DS3	0.40	—	—	40mBIG. Sandy component of Facies F1. Notable layering of coarser and finer grain sizes.
	US2-P1	0.29	DS2	0.26	6.0×10^{-4}	$\pm 1.8\times10^{-4}$	40mBIG. Gravel component of Facies F1, consisting of loosely cemented coarse sand to medium gravel, with some scattered coarser gravel sizes. Notable layering of coarser and finer grain sizes; sample breaks along weaker cemented layers.
	US5-P1	0.24	DS5	0.26	5.0×10^{-4}	$\pm 1.2\times10^{-4}$	40mBIG. Gravel component of Facies F1, consisting of coarse sand to fine gravel. Notable layering of coarser and finer grain sizes; sample breaks along weaker cemented layers..
	US11-P1	0.21	DS11	0.28	3.0×10^{-4}	$\pm 4.3\times10^{-5}$	Portal 1. Gravel component of Facies F1, consisting of coarse sand to medium gravel, with some scattered coarser gravel clasts.
	US1-P1	0.25	DS1	0.26	8.0×10^{-4}	$\pm 2.0\times10^{-4}$	40mBIG. Gravel component of Facies F1, consisting of coarse sand to coarse gravel. Notable layering of grain sizes within sample; breaks along coarser-grained, less cemented layers.
	US7-P1	0.25	DS7	0.26	5.0×10^{-4}	$\pm 7.2\times10^{-5}$	40mBIG. Gravel component of Facies F1, consisting of coarse sand to coarse gravel. Some distinct caliche nodules and layers of caliche.
	No sample		DS12	0.26	—	—	Portal 1. Moderately to poorly cemented fine to coarse gravel and sand. Coarser gravels were less well cemented.
	No sample		DS13	0.30	—	—	Portal 1. Low angle planar stratified fine to medium gravel.
	No sample		DS19	0.27	—	—	Near I-95. Poorly cemented fine to coarse gravel and sand.
	No sample		DS14	0.32	—	—	40mMED. Open-framework gravel from Facies F1.
	No sample		40mDS1-P1 40mDS1-P2 40mDS1-P3	— — —	2.2×10^{-3} 2.2×10^{-3} 2.3×10^{-3}	$\pm 2.2\times10^{-5}$ $\pm 8.0\times10^{-5}$ $\pm 8.6\times10^{-5}$	40mBIG. Fine to medium gravel with little to no sand.
	No sample		40mDS2-P1 40mDS2-P2 40mDS2-P3	— — —	4.8×10^{-5} 2.8×10^{-4} 1.7×10^{-4}	$\pm 2.7\times10^{-5}$ $\pm 8.9\times10^{-5}$ $\pm 4.2\times10^{-5}$	40mBIG. Fine to medium gravel with sand.
	No sample		40mDS5-P1 40mDS5-P2 40mDS5-P3	— — —	9.5×10^{-4} 5.8×10^{-4} 6.2×10^{-4}	$\pm 7.9\times10^{-5}$ $\pm 8.2\times10^{-5}$ $\pm 8.9\times10^{-5}$	40mBIG. Fine to medium gravel with sand.
	No sample		40mDS6-P1 40mDS6-P2 40mDS6-P3	— — —	4.4×10^{-4} 3.0×10^{-4} 3.4×10^{-4}	$\pm 4.6\times10^{-5}$ $\pm 3.4\times10^{-5}$ $\pm 5.7\times10^{-5}$	40mBIG. Coarse sand to fine gravel.
	No sample		40mDS8-P1 40mDS8-P2 40mDS8-P3	— — —	7.4×10^{-4} 3.1×10^{-4} 1.1×10^{-3}	$\pm 2.1\times10^{-5}$ $\pm 1.7\times10^{-5}$ $\pm 8.0\times10^{-5}$	40mBIG. Fine to medium gravel.
F2	US10-P1	0.29	DS10	0.40	9.0×10^{-5}	$\pm 3.9\times10^{-5}$	Portal 1. Sand matrix of Facies F2, consisting of very fine sand to fine sand with a few scattered gravel clasts.
F4	No sample		DS8	0.27	—	—	40mBIG. Fine to medium gravel with little sand.
	No sample		40mDS9-P1 40mDS9-P2 40mDS9-P3	— — —	2.6×10^{-4} 7.8×10^{-4} 3.7×10^{-4}	$\pm 1.6\times10^{-5}$ $\pm 7.2\times10^{-5}$ $\pm 4.5\times10^{-5}$	40mBIG. Fine to medium gravel with little sand.
F7	US6-P2 US6-P3	0.35 —	DS6	0.42	2.5×10^{-3} 2.0×10^{-4}	$\pm 1.9\times10^{-4}$ $\pm 3.0\times10^{-5}$	40mBIG. Well cemented fine sand with scattered fine gravel clasts
	US16-P1	—	DS16	0.26	7.0×10^{-4}	$\pm 1.0\times10^{-4}$	40mMED. Strongly cemented sand to coarse gravel. Notable layers of caliche.
	40mBIG-P12	0.32	No sample		3.0×10^{-4}	$\pm 1.4\times10^{-5}$	40mBIG. Strongly cemented sand to coarse gravel.
	No sample		40mDS7-P1 40mDS7-P2 40mDS7-P3	— — —	2.2×10^{-5} 5.4×10^{-6} 7.1×10^{-5}	$\pm 3.1\times10^{-6}$ $\pm 1.6\times10^{-6}$ $\pm 1.4\times10^{-5}$	40mBIG. Paleosol; predominantly medium sand.
	No sample		40mDS12-P1 40mDS12-P2 40mDS12-P3	— — —	1.9×10^{-5} 2.0×10^{-5} 3.4×10^{-5}	$\pm 3.3\times10^{-6}$ $\pm 3.9\times10^{-6}$ $\pm 8.0\times10^{-6}$	40mBIG. Paleosol; gravelly and strongly cemented.
F8	US4-P1	0.30	DS4	0.40	2.6×10^{-3}	$\pm 2.3\times10^{-4}$	40mBIG. Well cemented sand.
	US9-P1 US9-P2	0.36 0.30	DS9	0.41	6.0×10^{-4} 4.0×10^{-4}	$\pm 1.1\times10^{-4}$ $\pm 1.2\times10^{-4}$	Portal 1. Moderately cemented, medium to coarse sand with a few scattered gravel clasts.
	No sample		DS18	0.40	—	—	Near I-95. Poorly cemented medium to coarse sand with scattered gravel clasts.
	No sample		40mDS3-P1 40mDS3-P2 40mDS3-P3	— — —	2.0×10^{-5} 5.6×10^{-5} 3.3×10^{-5}	$\pm 5.7\times10^{-6}$ $\pm 5.4\times10^{-6}$ $\pm 9.0\times10^{-6}$	40mBIG. Cross-stratified medium to coarse sand.

Table 3. Saturated hydraulic conductivity (K_{sat}) derived from empirical grain-size-permeability relations presented in Shepherd (1989) and Vukovic and Soro (1992). The relations from Vukovic and Soro (1992) include a porosity factor; therefore, the K_{sat} was calculated using both the laboratory-derived porosity (LP) and the grain-size-derived porosity (GSP) to evaluate sensitivity of the relations to the porosity estimate. The empirical relations have a domain of applicability based on grain size, and the K_{sat} values developed from an empirical relation outside the domain of applicability are shown in parentheses.

		K_{sat} estimates (cm/s) using relations from Shepherd (1989)						K_{sat} estimates (cm/s) using relations from Vukovic and Soro (1992) and either laboratory-derived porosity (LP) or grain size-derived porosity (GSP)															
Empirical relation:		Krumbein & Monk	Bedinger	Keech & Rosene	Masch & Denny	Mavis & Wilsey	Shepherd	Hazen		Slichter		Terzaghi		Beyer		Krüger		Kozeny		Zunker		Zamarin		USBR	
Sediment type of data set or applicability limits:		Outwash	River alluvium	River alluvium	River sand fractions	River sand	Immature sediment	$0.1 < d_e < 3$ mm $C_u < 5$		$0.01 < d_e < 5$ mm		Large-grain sands		$0.06 < d_e < 0.6$ mm $1 < C_u < 20$		Medium-grain sands $C_u > 5$		Large-grain sands		Fine and medium-grain sands		Large-grain sands		Medium-grain sands $C_u < 5$	
Facies	**Sediment Sample**							LP	GSP	LP	GSP	LP	GSP	LP	GSP	LP	GSP	LP	GSP	LP	GSP	LP	GSP	LP	GSP
F1	DS17	1.4×10^{2}	1.6×10^{2}	3.5×10^{2}	(3.1×10^{2})	(5.0×10^{2})	1.2×10^{2}	2.4×10^{2}	2.7×10^{2}	6.7×10^{3}	8.5×10^{3}	1.2×10^{2}	1.5×10^{2}	2.3×10^{2}	2.3×10^{2}	(1.6×10^{3})	(1.9×10^{3})	3.3×10^{2}	4.4×10^{2}	1.4×10^{2}	1.8×10^{2}	2.0×10^{2}	2.4×10^{2}	3.2×10^{2}	3.2×10^{2}
	DS3	7.7×10^{3}	1.1×10^{2}	2.0×10^{2}	(2.1×10^{2})	(2.9×10^{2})	8.1×10^{3}	—	2.1×10^{2}	—	7.3×10^{3}	—	1.3×10^{2}	—	1.7×10^{2}	—	(9.1×10^{5})	—	8.5×10^{4}	—	4.7×10^{4}	—	9.2×10^{4}	—	1.4×10^{2}
	DS2	3.0×10^{1}	1.6×10^{1}	8.2×10^{1}	(2.9×10^{1})	(1.1×10^{0})	1.3×10^{1}	1.6×10^{2}	1.2×10^{2}	3.4×10^{3}	2.4×10^{3}	5.4×10^{3}	3.5×10^{3}	(1.5×10^{2})	(1.5×10^{2})	6.2×10^{4}	5.2×10^{4}	8.8×10^{3}	6.0×10^{3}	4.6×10^{3}	3.4×10^{3}	6.8×10^{3}	5.1×10^{3}	(5.9×10^{2})	(5.9×10^{2})
	DS5	1.4×10^{1}	9.3×10^{2}	3.8×10^{1}	(1.7×10^{1})	(5.2×10^{1})	7.4×10^{2}	7.2×10^{3}	9.9×10^{3}	1.4×10^{3}	2.0×10^{3}	1.8×10^{3}	2.9×10^{3}	1.2×10^{2}	1.2×10^{2}	6.1×10^{4}	7.4×10^{4}	5.6×10^{3}	8.6×10^{3}	3.6×10^{3}	4.9×10^{3}	5.3×10^{3}	7.2×10^{3}	(2.9×10^{2})	(2.9×10^{2})
	DS11	2.8×10^{1}	1.6×10^{1}	7.7×10^{1}	(2.7×10^{1})	(1.0×10^{0})	1.3×10^{1}	1.5×10^{2}	4.0×10^{2}	3.1×10^{3}	8.5×10^{3}	3.2×10^{3}	1.3×10^{2}	4.6×10^{2}	4.6×10^{2}	6.1×10^{4}	1.0×10^{3}	4.4×10^{3}	1.3×10^{2}	3.2×10^{3}	7.2×10^{3}	4.5×10^{3}	1.1×10^{2}	(1.2×10^{1})	(1.2×10^{1})
	DS1	1.6×10^{0}	5.8×10^{1}	4.5×10^{0}	(9.6×10^{1})	(6.0×10^{0})	4.8×10^{1}	1.3×10^{2}	1.3×10^{2}	2.5×10^{3}	2.6×10^{3}	3.5×10^{3}	3.8×10^{3}	(1.2×10^{2})	(1.2×10^{2})	7.8×10^{5}	8.0×10^{5}	2.4×10^{5}	2.6×10^{5}	4.2×10^{5}	4.4×10^{5}	2.9×10^{4}	3.0×10^{4}	(7.6×10^{2})	(7.6×10^{2})
	DS7	6.1×10^{1}	2.8×10^{1}	1.7×10^{0}	(4.8×10^{1})	(2.2×10^{0})	2.3×10^{1}	1.5×10^{2}	1.7×10^{2}	2.9×10^{3}	3.4×10^{3}	4.0×10^{3}	4.8×10^{3}	(1.9×10^{2})	(1.9×10^{2})	3.5×10^{3}	3.8×10^{3}	3.4×10^{2}	4.0×10^{2}	2.1×10^{2}	2.4×10^{2}	3.1×10^{2}	3.6×10^{2}	(7.1×10^{2})	(7.1×10^{2})
	DS12	9.2×10^{1}	3.8×10^{1}	2.6×10^{0}	(6.5×10^{1})	(3.4×10^{0})	3.1×10^{1}	—	4.2×10^{2}	—	8.3×10^{3}	—	1.2×10^{2}	—	(5.0×10^{2})	—	1.1×10^{3}	—	1.3×10^{2}	—	7.4×10^{3}	—	1.1×10^{2}	—	(1.7×10^{1})
	DS13	5.8×10^{1}	2.7×10^{1}	1.6×10^{0}	(4.6×10^{1})	(2.1×10^{0})	2.2×10^{1}	—	1.3×10^{1}	—	3.1×10^{2}	—	5.0×10^{2}	—	1.4×10^{1}	—	1.6×10^{3}	—	2.5×10^{2}	—	1.2×10^{2}	—	1.8×10^{2}	—	(6.8×10^{1})
	DS19	4.3×10^{1}	2.1×10^{1}	1.2×10^{0}	(3.7×10^{1})	(1.6×10^{0})	1.7×10^{1}	—	5.8×10^{2}	—	1.2×10^{2}	—	1.8×10^{2}	—	7.0×10^{2}	—	9.9×10^{3}	—	1.2×10^{1}	—	6.5×10^{2}	—	9.9×10^{2}	—	(1.8×10^{1})
	DS14	1.2×10^{0}	4.7×10^{1}	3.5×10^{0}	(8.0×10^{1})	(4.6×10^{0})	3.9×10^{1}	—	6.1×10^{1}	—	1.5×10^{1}	—	2.5×10^{1}	—	(6.0×10^{1})	—	5.9×10^{3}	—	1.1×10^{1}	—	4.9×10^{2}	—	7.1×10^{2}	—	(2.4×10^{0})
F2	DS10	1.2×10^{3}	2.7×10^{3}	3.1×10^{3}	5.6×10^{3}	4.6×10^{3}	2.0×10^{3}	1.8×10^{3}	3.3×10^{3}	3.9×10^{4}	1.1×10^{3}	6.2×10^{4}	2.0×10^{3}	2.6×10^{3}	2.6×10^{3}	(4.0×10^{5})	(7.7×10^{5})	5.0×10^{4}	1.8×10^{3}	2.8×10^{4}	7.3×10^{4}	4.1×10^{4}	9.7×10^{4}	1.6×10^{3}	1.6×10^{3}
F4	DS8	5.4×10^{1}	2.5×10^{1}	1.5×10^{0}	(4.4×10^{1})	(2.0×10^{0})	2.1×10^{1}	—	3.4×10^{2}	—	6.9×10^{3}	—	1.0×10^{2}	—	4.1×10^{2}	—	3.3×10^{3}	—	3.8×10^{2}	—	2.2×10^{2}	—	3.3×10^{2}	—	(1.8×10^{1})
F7	DS6	2.4×10^{3}	4.4×10^{3}	6.1×10^{3}	9.0×10^{3}	8.9×10^{3}	3.3×10^{3}	7.7×10^{3}	1.0×10^{2}	2.2×10^{3}	3.9×10^{3}	3.7×10^{3}	6.8×10^{3}	8.2×10^{3}	8.2×10^{3}	(4.3×10^{4})	(6.4×10^{4})	8.4×10^{3}	1.8×10^{2}	3.7×10^{3}	6.6×10^{3}	5.3×10^{3}	8.4×10^{3}	4.8×10^{3}	4.8×10^{3}
	DS16	9.5×10^{2}	6.9×10^{2}	2.6×10^{1}	(1.3×10^{1})	(3.5×10^{1})	5.5×10^{2}	—	6.6×10^{3}	—	1.3×10^{3}	—	1.9×10^{3}	—	7.9×10^{3}	—	1.0×10^{4}	—	1.9×10^{5}	—	3.7×10^{5}	—	3.8×10^{4}	—	(2.1×10^{2})
F8	DS4	6.3×10^{3}	9.1×10^{3}	1.6×10^{2}	1.8×10^{2}	2.3×10^{2}	6.9×10^{3}	1.0×10^{2}	1.7×10^{2}	2.3×10^{3}	5.8×10^{3}	3.8×10^{3}	1.0×10^{2}	1.4×10^{2}	1.4×10^{2}	(7.6×10^{4})	(1.4×10^{3})	1.1×10^{2}	3.5×10^{2}	5.7×10^{3}	1.3×10^{2}	8.5×10^{3}	1.8×10^{2}	1.1×10^{2}	1.1×10^{2}
	DS9	4.2×10^{3}	6.6×10^{3}	1.1×10^{2}	1.3×10^{2}	1.5×10^{2}	5.0×10^{3}	1.3×10^{2}	1.6×10^{2}	3.8×10^{3}	5.7×10^{3}	6.6×10^{3}	1.0×10^{2}	1.3×10^{2}	1.3×10^{2}	(1.3×10^{4})	(1.8×10^{4})	2.8×10^{4}	4.6×10^{4}	2.5×10^{4}	3.7×10^{4}	9.2×10^{4}	1.3×10^{3}	7.2×10^{3}	7.2×10^{3}
	DS18	4.7×10^{3}	7.3×10^{3}	1.2×10^{2}	1.4×10^{2}	1.7×10^{2}	5.5×10^{3}	—	1.4×10^{2}	—	4.9×10^{3}	—	8.5×10^{3}	—	1.1×10^{2}	—	(1.4×10^{3})	—	3.7×10^{2}	—	1.4×10^{2}	—	1.9×10^{2}	—	7.1×10^{3}

Notes:
d_e = effective grain diameter
C_u = uniformity coefficient

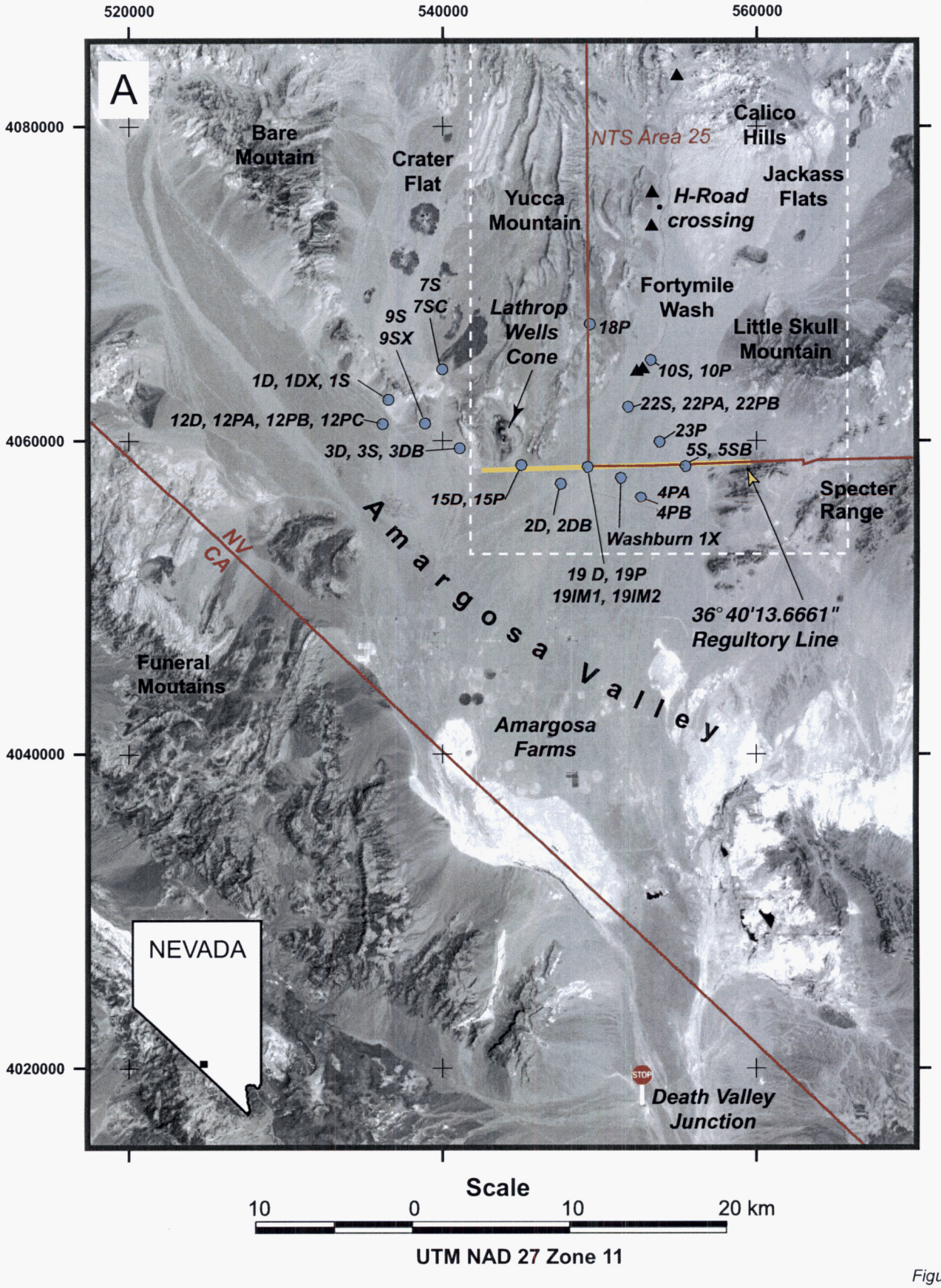

Figure 1a
Ressler et al.

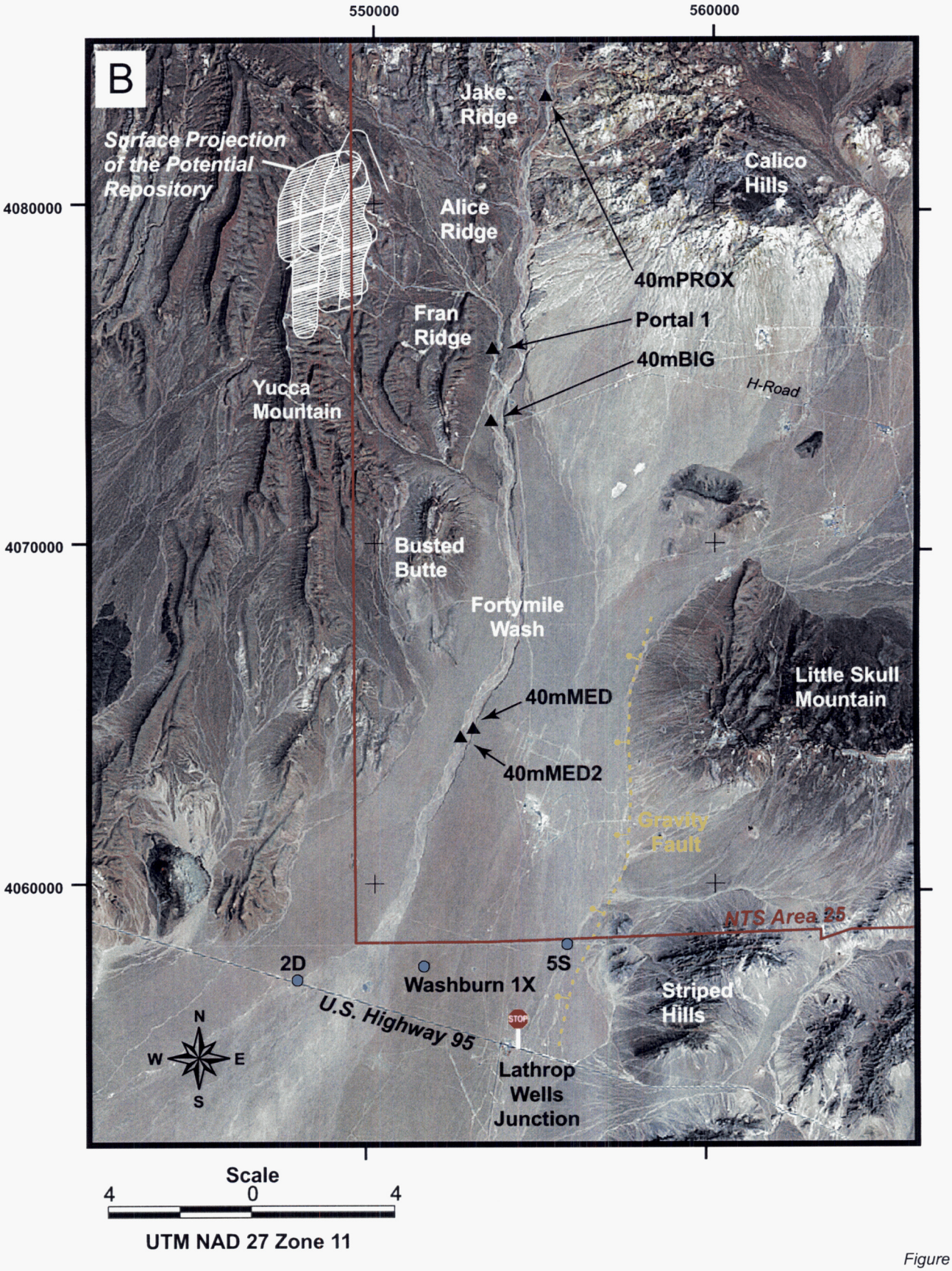

Figure 1b
Ressler et al.

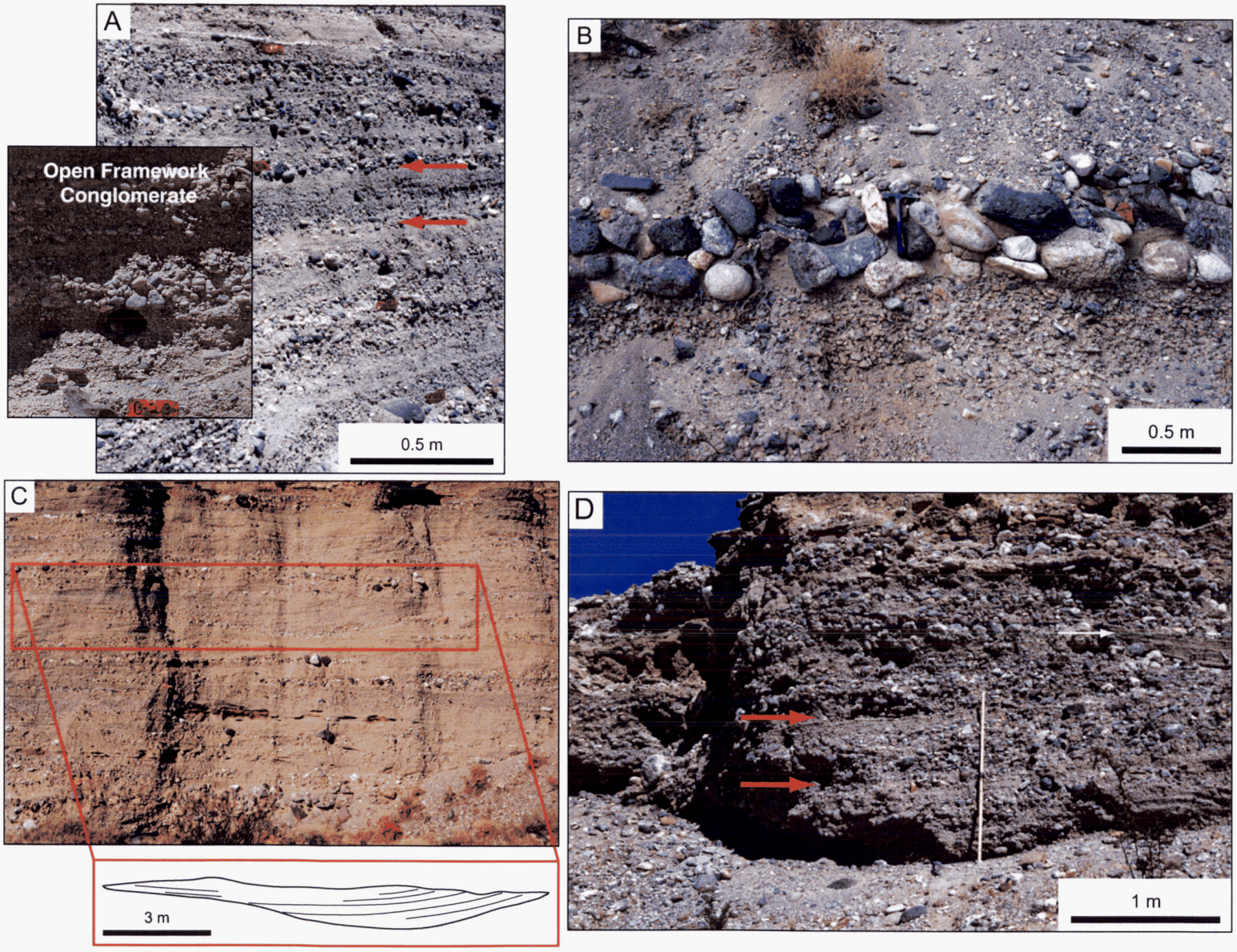

Figure 2
Ressler et al.

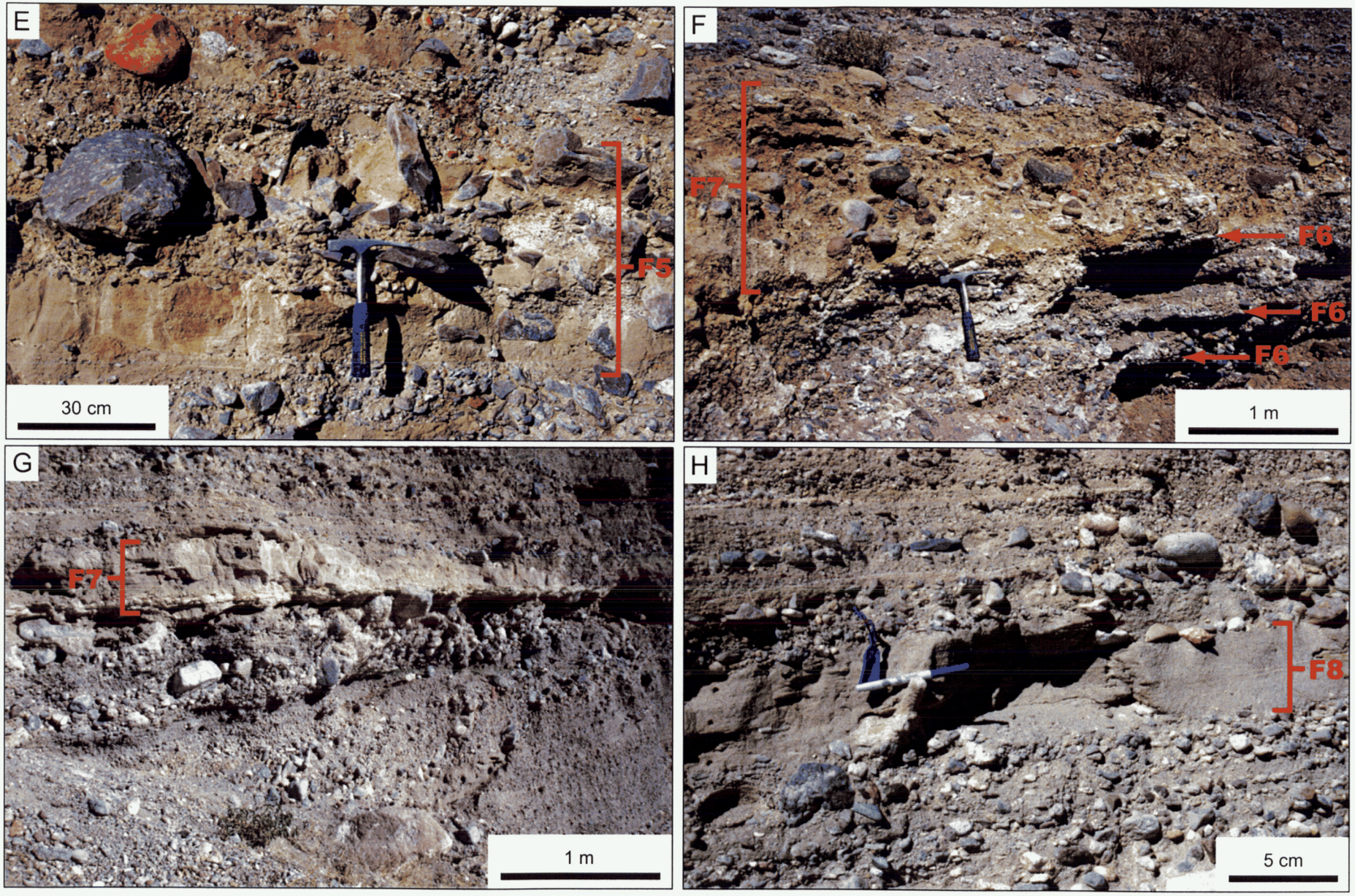

Figure 2 con't.
Ressler et al.

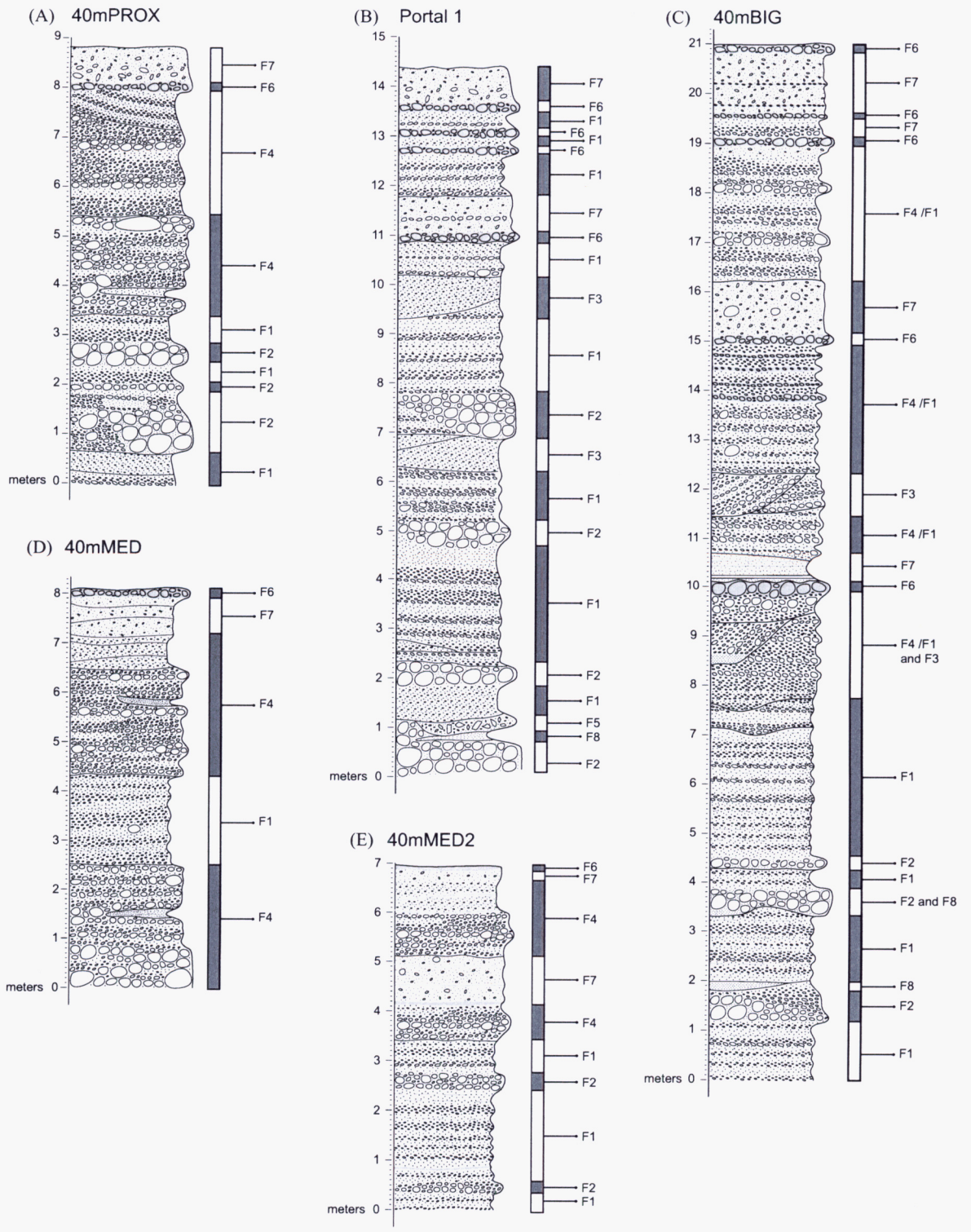

Figure 3
Ressler et al.

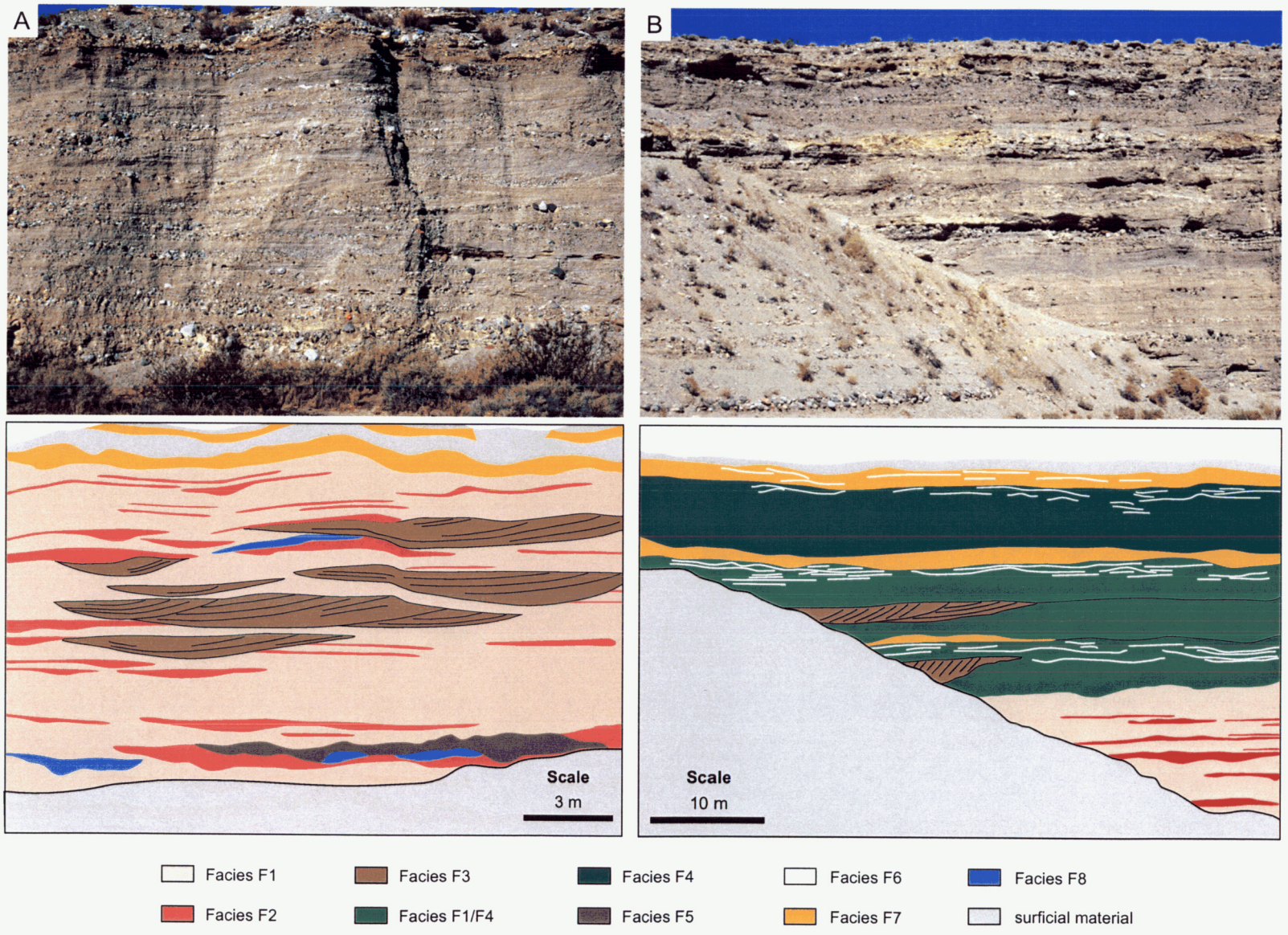

Figure 4
Ressler et al.

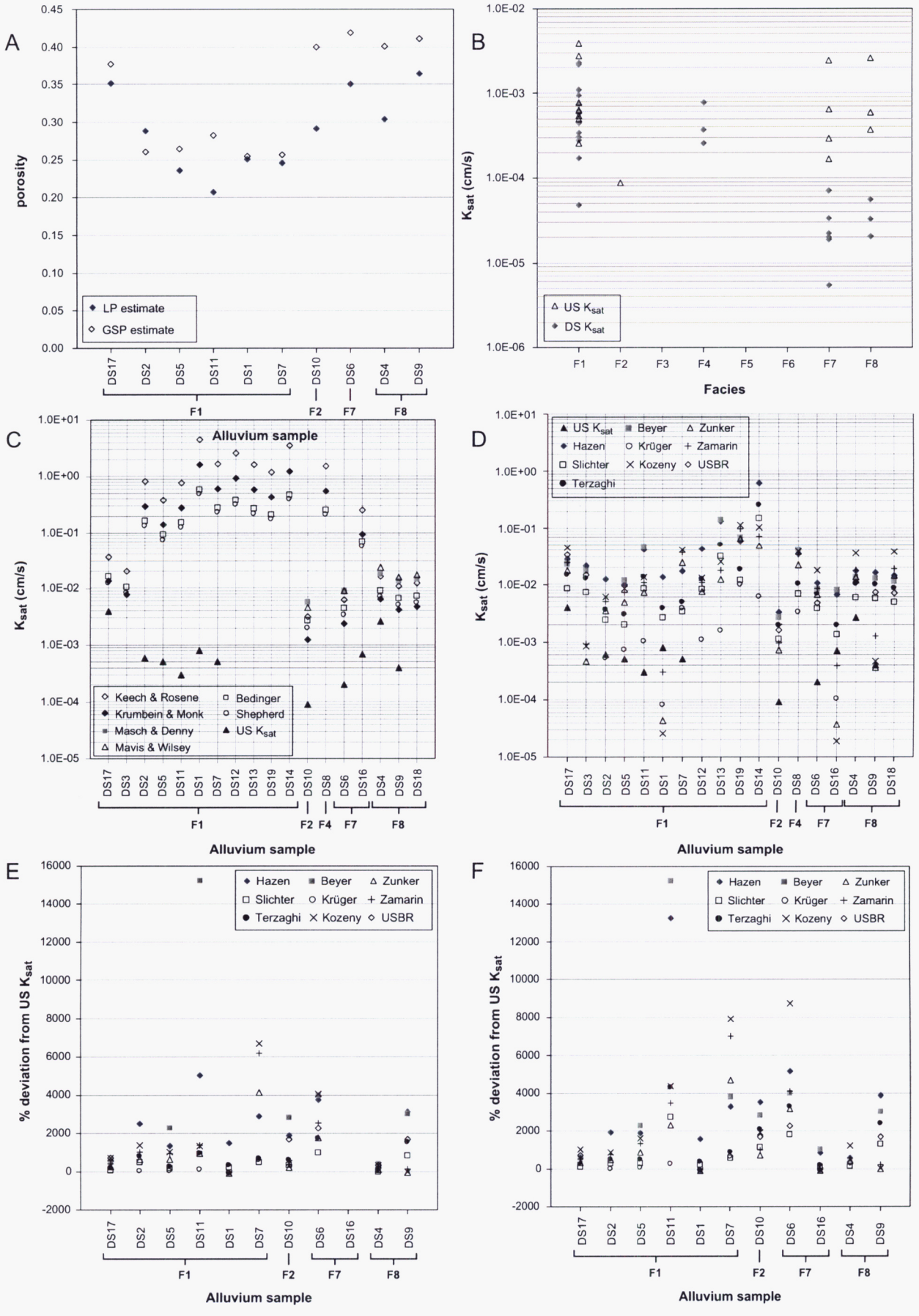

Figure 5
Ressler et al.